

# Generalized Feistel Ciphers for Efficient Prime Field Masking - Full Version

Lorenzo Grassi<sup>1</sup>, Loïc Masure<sup>2</sup>, Pierrick Méaux<sup>3</sup>,  
Thorben Moos<sup>4</sup>, François-Xavier Standaert<sup>4</sup>

<sup>1</sup> Ruhr University Bochum, Bochum, Germany

<sup>2</sup> LIRMM, Univ. Montpellier, CNRS

<sup>3</sup> Luxembourg University, Esch-sur-Alzette, Luxembourg

<sup>4</sup> Crypto Group, ICTEAM Institute, UCLouvain, Louvain-la-Neuve, Belgium

**Abstract** A recent work from Eurocrypt 2023 suggests that prime-field masking has excellent potential to improve the efficiency vs. security tradeoff of masked implementations against side-channel attacks, especially in contexts where physical leakages show low noise. We pick up on the main open challenge that this seed result leads to, namely the design of an optimized prime cipher able to take advantage of this potential. Given the interest of tweakable block ciphers with cheap inverses in many leakage-resistant designs, we start by describing the FPM (Feistel for Prime Masking) family of tweakable block ciphers based on a generalized Feistel structure. We then propose a first instantiation of FPM, which we denote as `small-pSquare`. It builds on the recent observation that the square operation (which is non-linear in  $\mathbb{F}_p$ ) can lead to masked gadgets that are more efficient than those for multiplication, and is tailored for efficient masked implementations in hardware. We analyze the mathematical security of the FPM family of ciphers and the `small-pSquare` instance, trying to isolate the parts of our study that can be re-used for other instances. We additionally evaluate the implementation features of `small-pSquare` by comparing the efficiency vs. security tradeoff of masked FPGA circuits against those of a state-of-the-art binary cipher, namely SKINNY, confirming significant gains in relevant contexts.

## 1 Introduction

The design of symmetric cryptographic algorithms is generally oriented towards optimizing their efficiency vs. security tradeoff. For most general applications, this has led researchers to focus primarily on binary ciphers with efficient bit-slice implementations, which are generally efficient in software [19] and hardware [79]. This trend has even been amplified when considering side-channel attacks, in good part due to the emergence of masking as the most popular solution to mitigate such attacks. While various types of masking schemes exist (e.g., additive [36], multiplicative [64], affine [63], polynomial [99], inner product [5], code-based [115]), the efficiency of Boolean masked implementations in software [65] and hardware [71] make it for now a default solution. As a result,

ciphers optimized towards low AND complexity, enabling efficient bit-oriented implementation (e.g., bitslicing), appeared for a while as the best approach [72]. This situation is also reflected by the recent NIST Lightweight Cryptography standardization effort, where most ciphers designed with leakage in mind (including the winner Ascon [50]) have efficient bitslice representations.<sup>1</sup>

While it has been shown that Boolean masking can bring high security at limited cost, it is also known to suffer from practical limitations. Among others, it is only effective in contexts where leakages are sufficiently noisy [98,52,53], a condition that was shown to be challenging to reach without dedicated noise generation circuitry, both in software [7,30] and in hardware [97,93]. Building on theoretical advances of Dziembowski et al. [57], it has then been observed that computing in groups of prime order can significantly reduce the noise requirements of masking security proofs while keeping most of the benefits of additive encodings, and even providing security gains in the context of noisy leakages (that were not covered by theoretical analysis) [90]. More precisely, Masure et al. showed at Eurocrypt 2023 that for concretely-relevant leakage functions, prime-field masking can be quite efficient by re-using simple additions and multiplication algorithms “à la ISW” [76], and that the mild performance overheads due to operating in prime fields can be largely compensated by concrete side-channel security gains. Informally, these gains can be viewed as the result of a decreased “algebraic compatibility” between the leakage functions observed in practice (which are typically close to a linear combination of bits [101]) and the field in which we mask. For example, it is well-known that observing the least significant bit of Hamming weight leakages obtained from Boolean shares leads to information about the secret independent of the number of shares [105]. Moving to prime encodings, such an attack is not directly possible anymore because partial uncertainty “diffuses” better when combining the shares.

So far, this potential advantage of prime-field masking for counteracting side-channel attacks was only demonstrated for a toy AES-like cipher. The main open challenge that we pick up in this paper is, thus, the design of a dedicated lightweight cipher optimized for prime masking to enable fair comparisons with binary ciphers which are tailored for cost-efficiency when masked.

Given the interest of Tweakable Block Ciphers (TBCs) with cheap inverse for leakage-resistant modes of operation [9,12], we start by describing the FPM (Feistel for Prime Masking) family of tweakable block ciphers based on a generalized Feistel structure [96,74]. Among other advantages, TBCs allow reducing the need of idealized assumptions that are hard to justify in physical security analyzes and to minimize the side-channel attack surface during tag verification (which can leak in an unbounded manner thanks to the inverse trick of [13]). The FPM family of ciphers allows tweaks of variable size including a version without tweak (i.e., a block cipher, in order to enable comparisons with generic constructions [114]). It relies on a variant of the TWEAKEY framework [78], taking advantage of the fact that for most leakage-resistant modes of operation, the tweak is public information and requires no countermeasures (so we can ac-

<sup>1</sup> <https://csrc.nist.gov/Projects/lightweight-cryptography>

tually use a simple key scheduling algorithm and a more complex, non-linear, tweak scheduling algorithm). While moving towards a first instantiation of FPM, we additionally exploit recent results from CHES 2023 which show how to obtain a secure implementation of the square operation (non-linear in  $\mathbb{F}_p$ ) which is more efficient than a secure multiplication [33]. This provides natural incentive for designing a cipher using the square operation as only source of non-linearity, which further motivates the use of Feistel-like structures for FPM TBCs and their underlying building blocks, since the square is also non-invertible in  $\mathbb{F}_p$ . What then mostly remains is to choose the prime number defining the field in which we operate. Following [90], we use a Mersenne prime for efficiency reasons.<sup>2</sup> We set this modulus to  $2^7 - 1$  in order to propose an instance tailored for secure hardware implementation, which we denote as **small-pSquare**.

Besides defining the FPM family of ciphers and a first instance, we provide an initial mathematical security analysis in order to select the number of cipher rounds of **small-pSquare**. Doing so, we try to separate the parts of the analysis that are generic (and could be re-used for other instances) from the ones that are linked to our choice of square S-box and 7-bit prime. Most importantly, we then compare masked FPGA implementations of **small-pSquare** and similar implementations of a binary cipher protected with Boolean masking. We use **SKINNY** for this purpose [8], which is a popular family of ciphers with tweakable versions that amongst other applications was used in Romulus, a finalist to NIST lightweight cryptography competition, and for which a rich literature on the construction and analysis of state-of-the-art Boolean masked implementations exist, both automated [80] and hand-made [111]. Our experiments allow us to confirm the excellent performances and significantly improved efficiency vs. (side-channel) security tradeoff for **small-pSquare**. We show in Section 6 that while unprotected **small-pSquare** implementations come with overheads (compared to **SKINNY**), these overheads vanish in the context of masked implementations where both algorithms perform similarly. As expected, **small-pSquare** also has significantly improved performances compared to the toy AES-like cipher considered in [90]. Furthermore, we show in Section 7 that for similar architectures, **small-pSquare** offers side-channel security levels which exceed those of masked **SKINNY** implementations by (at least) one order of magnitude.

We conclude the paper by discussing scopes for further research and other instances of FPM ciphers. First, considering different implementation contexts, for example **mid-pSquare** variants could be relevant to investigate for FPGAs with DSP blocks (e.g., with a 17-bit prime) or for ARM Cortex-like devices (e.g., with a 31-bit prime). Second, and more prospectively, **big-pSquare** variants (with larger primes) could be of interest conceptually due to their similarity with the different prime ciphers developed for other applications (e.g., fully-homomorphic encryption, multi-party computation, zero-knowledge proofs), in order to better understand the differences and similarities between the design goals to optimize

---

<sup>2</sup> Both because such prime numbers allow very efficient modular reductions and because the  $x \mapsto 2x$  operation is a rotation of the bits that is free in hardware.

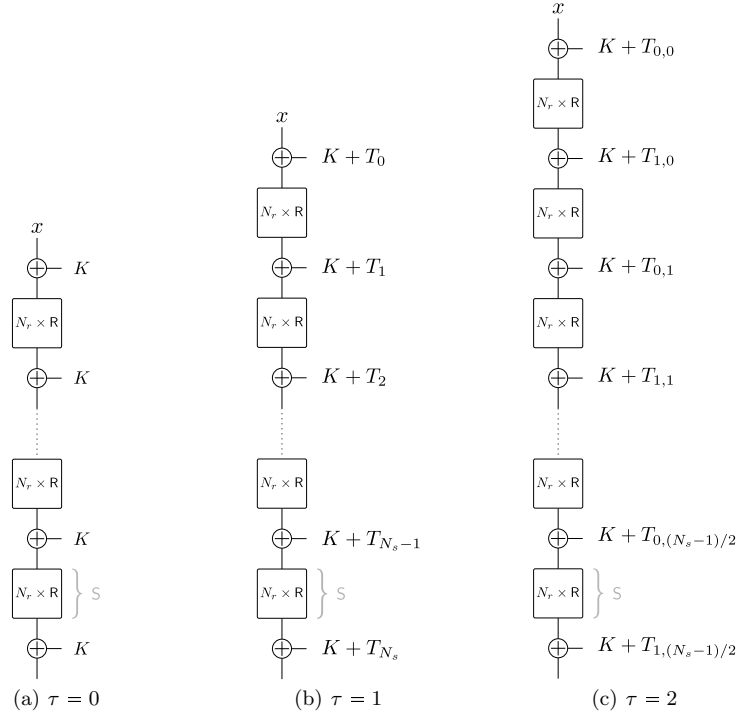


Figure 1: High-level view of FPM (tweakable) ciphers. We use the shortcut notation  $N_r \times R$  to denote the application of the round  $R$   $N_r$  times.

for these various applications [2,1,3,68,51,38], and possibly to offer stronger physical security guarantees thanks to the larger field computations [56].

## 2 Feistel for Prime Masking

In this section, we introduce the  $\text{FPM}_\tau$  family of TBCs. We start by describing the high-level Feistel structure we use in Section 2.1. We then detail the internal components of this structure in Sections 2.2 and 2.3. We conclude by summarizing the design space that this family of ciphers defines in Section 2.4.

### 2.1 High-Level Structure

Let  $p \geq 3$  be a prime number, and let  $n = 2 \cdot n' \geq 4$  be an integer. The high-level structure of  $\text{FPM}_\tau$  TBCs is given in Figure 1.  $\text{FPM}_\tau$  ciphers take as inputs a plaintext  $x \in \mathbb{F}_p^n$ , a key  $K \in \mathbb{F}_p^n$  and an optional tweak defined as:

$$T := \begin{cases} (T^{(1)}, T^{(2)}, \dots, T^{(\tau)}) \in \mathbb{F}_p^{\tau n} & \text{if } \tau \geq 1 \\ \emptyset & \text{otherwise } (\tau = 0) \end{cases}.$$

If  $\tau = 0$ , then  $\text{FPM}_0$  ciphers receive no tweak input and correspond to block ciphers.  $\text{FPM}_\tau$  ciphers are key alternating ciphers, where a tweakkey is added every  $r > 1$  rounds. We denote a single round as  $\text{R}$ , and we denote a group of  $N_r$  rounds  $\text{R}$  as a step  $\text{S}$ . A tweakkey addition is performed after every step. If  $\tau = 0$ , the tweakkey is always the master key  $K$ . If  $\tau \geq 1$ , the tweakkeys are defined as  $K + T_{0,0}, K + T_{1,0}, \dots, K + T_{\tau-1,0}, K + T_{0,1}, K + T_{1,1}, \dots, K + T_{\tau-1,1}, \dots, K + T_{0,i}, K + T_{1,i}, \dots, K + T_{\tau-1,i}$ , where the values  $T_{j,i} \in \mathbb{F}_p^n$  are produced by a tweak scheduling and are independent of the master key. If  $\tau = 1$ , we usually omit the first index for simplicity (i.e., we use  $T_i$  instead of  $T_{0,i}$ ).

The rounds  $\text{R} : \mathbb{F}_p^n \rightarrow \mathbb{F}_p^n$  (and the steps  $\text{S}$ ) are independent of both the tweak and of the master key. The number of rounds per step  $N_r$  must at least guarantee that full diffusion is achieved in the steps. Regarding the number of steps  $N_s$ , we additionally require that if  $\tau \geq 1$ , then  $N_s - 1$  must be a multiple of  $\tau$  in order to guarantee that the tweak is absorbed in equal measure.

**Key and tweak scheduling algorithms.** Since we do not claim security against related-key attacks, we opted for the simplest key scheduling algorithm, which consists of having all the subkeys equal to the master key. Note that several tweakable lightweight symmetric primitives in the literature are based on similar design choices, including `SKINNY` [8] (which we will use in our comparisons).

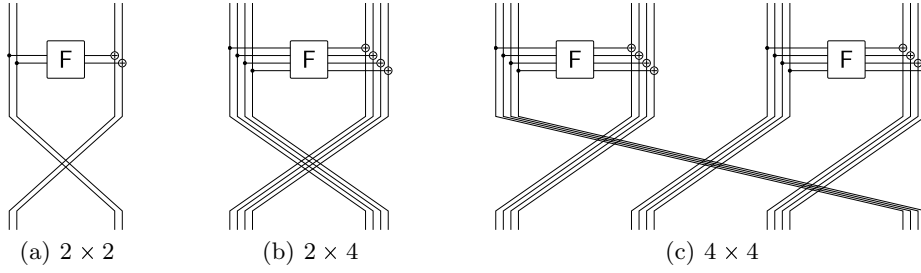
By contrast, our designs make use of a tweak scheduling algorithm. As mentioned in the introduction, this is because in many leakage-resistant modes of operation, the tweak is public and therefore does not require any protection against leakage. This context calls for operations that are cheap to implement without countermeasures (in hardware and software) while providing good cryptographic properties. Since  $\text{FPM}$  ciphers operate in prime fields, a natural candidate for this purpose is to combine a shuffling of the  $\mathbb{F}_p$ -words in each state with an invertible mapping of the “bits” in each  $\mathbb{F}_p$ -word, for example taking advantage of the fact that linear mappings in  $\mathbb{F}_2$  are non-linear in  $\mathbb{F}_p$ . More precisely, for each  $i \geq 0$  and for each  $j \in \{0, 1, \dots, \tau - 1\}$ , we define  $T_{j,i}$  as:

$$T_{j,i} := \Psi_0 \left( T_{\Pi^i(0)}^{(j)} \right) \parallel \Psi_1 \left( T_{\Pi^i(1)}^{(j)} \right) \parallel \dots \parallel \Psi_{n-1} \left( T_{\Pi^i(n-1)}^{(j)} \right) \in \mathbb{F}_p^n,$$

where:

- For each  $l \in \{0, 1, \dots, n - 1\}$ ,  $T_l^{(j)} \in \mathbb{F}_p$  denotes the  $l$ -th  $\mathbb{F}_p$ -word of  $T^{(j)}$ ;
- $\Pi$  is a shuffling of  $\{0, 1, \dots, n - 1\} \subseteq \mathbb{N}$  satisfying the following conditions:
  1.  $\Pi^i$  (where  $\Pi^i$  denotes the application of  $\Pi$   $i$  consecutive times) is different from the identity for each  $i \leq i'$  and a sufficiently large  $i'$ ;
  2.  $\Pi$  does not contain fix points and (if possible) two consecutive elements before the shuffling are not consecutive after it.
- For each  $l \in \{0, 1, \dots, n - 1\}$ ,  $\Psi_l : \mathbb{F}_p \rightarrow \mathbb{F}_p$  is an invertible mapping.

As we are going to show in the next section, this tweak scheduling algorithm allows us to adapt the simple security arguments used in [73] to our scheme.

Figure 2: FPM rounds. Left:  $b=2, c=2$ ; middle:  $b=2, c=4$ ; right:  $b=4, c=4$ .

## 2.2 Rounds R of $\text{FPM}_\tau$ via Type-II Generalized Feistel

Let  $b, c \geq 2$  be positive integers such that  $n = b \cdot c$  and  $b = 2 \cdot b'$ . The rounds R over  $(\mathbb{F}_p^c)^b \equiv \mathbb{F}_p^n$  of  $\text{FPM}_\tau$  ciphers are based on a Type-II generalized Feistel network structure [116,96,74]. They are defined as:

$$(x_0, x_1, \dots, x_{b-2}, x_{b-1}) \mapsto (F(x_0) + x_1, x_2, F(x_2) + x_3, \dots, F(x_{b-2}) + x_{b-1}, x_0),$$

where  $F : \mathbb{F}_p^c \equiv \mathbb{F}_{p^c} \rightarrow \mathbb{F}_p^c \equiv \mathbb{F}_{p^c}$  is discussed in the next subsection. Such structures are characterized by two parameters:  $b = 2 \cdot b' \geq 2$  is the number of branches in the generalized Feistel network (where each branch can carry several values in  $\mathbb{F}_p$ ),  $c \geq 2$  is the number of values in  $\mathbb{F}_p$  of each branch, that the non-linear F function takes as input. Figure 2 illustrates three examples.

**Remark: Achieving faster diffusion.** In this paper, we limit ourselves to instances with small  $b$  values (up to 4) and to the classical Type-II generalized Feistel scheme, in which a shift is applied at the output of the non-linear layer. However, several studies have been conducted in literature to find better shuffles of the words that can achieve faster diffusion for larger  $b$  values (see for example [108,35]), which we suggest to use in place of the shift whenever applicable. Besides the minimum number of rounds necessary for achieving full diffusion, these references also provide the number of active functions F.

## 2.3 Function F of the Type-III Generalized Feistel

The F functions over  $\mathbb{F}_p^c$  are designed to 1) be bijective (since collisions at their outputs could make the security analysis harder) and 2) ensure full non-linear diffusion. This is achieved by combining the following components:

- A first non-linear layer is instantiated via a Type-III generalized Feistel network [116,96,74] (without the shift) of the form:  $(x_0, x_1, x_2, \dots, x_{c-1}) \in \mathbb{F}_p^c \mapsto (x_0, G_{0,0}(x_0) + x_1, G_{1,0}(x_1) + x_2, \dots, G_{c-2,0}(x_{c-2}) + x_{c-1}) \in \mathbb{F}_p^c$ , where  $G_{0,0}, G_{1,0}, \dots, G_{c-2,0}$  are non-linear operations over  $\mathbb{F}_p$ .

- The non-linear layer is followed by a multiplication with a  $c \times c$  Maximum Distance Separable (MDS) matrix [47,48], typically lightweight [88,82,55].<sup>3</sup>
- Finally, a non-linear layer instantiated via a Type-III generalized Feistel network (with the shift) is applied to the state:  $(x_0, x_1, x_2, \dots, x_{c-1}) \in \mathbb{F}_p^c \mapsto (x_0, \mathbf{G}_{0,1}(x_0) + x_1, \mathbf{G}_{1,1}(x_1) + x_2, \dots, \mathbf{G}_{c-2,1}(x_{c-2}) + x_{c-1}) \in \mathbb{F}_p^c$ , where  $\mathbf{G}_{0,0}, \mathbf{G}_{1,0}, \dots, \mathbf{G}_{c-2,0}$  are again non-linear operations over  $\mathbb{F}_p$ .

Before the application of each Type-III generalized Feistel network, a round constant is added on the first element  $x_0$ . We suggest to generate these constants via bit rotations of a mathematical constant as  $\pi = 3.14159\dots \in \mathbb{R}$  rounded to a bit size that is large enough to avoid cycles for the number of cipher rounds.

We note that using a Type-III generalized Feistel network for the  $\mathbf{F}$  functions is motivated by the fact that a potential candidate for the  $\mathbf{G}_{i,j}$  functions is the square operation which is non-invertible (or other small power maps which are non-bijective in the respective field). In case the  $\mathbf{G}_{i,j}$  functions are themselves bijective, a simpler alternative is to directly use SPN rounds.

We also note that since we use a bijective  $\mathbf{F}$ , exploiting a Feistel structure for the rounds of Section 2.2 is not mandatory (e.g., an SPN could work there too). However, it has the advantage that the  $\mathbf{F}$  function can be chosen without any regard for the implementation efficiency of its inverse (with or without masking), which would not be the case when used as an S-box in a typical SPN construction. Furthermore, the Feistel strategy directly enables us to obtain cheap inverses in the sense that 1) cost of decryption  $\approx$  cost of encryption and 2) implementing a hardware circuit that can both encrypt and decrypt is not (significantly) more expensive than one which can only encrypt (in contrast to most standard SPN designs). In general, we believe that the high-level structure of FPM ciphers is a natural starting point given our goals. SPN-based structures would also require an additional linear layer (which may be more expensive) and it is unclear whether it would enable a reduction of the number of rounds by half (to compensate for the cost of operating on the full state in each round). Yet, investigating whether such prime SPN ciphers could potentially improve over the proposed FPM designs remains an interesting open problem.

## 2.4 Summary of the $\text{FPM}_\tau$ Design Space

The size of an  $\text{FPM}_\tau$  cipher is determined by the number of tweaks  $\tau$ , the prime integer  $p$ , the number of branches of the Type-II generalized Feistel network  $b$  and the number of input words of the  $\mathbf{F}$  functions  $c$ . We use the notation  $\text{FPM}_\tau(\rho, b, c)$  for this purpose, where  $\rho = \lceil \log_2(p) \rceil$ . The cipher specifications additionally require to choose the functions  $\mathbf{G}_{i,j} : \mathbb{F}_p \rightarrow \mathbb{F}_p$  and an MDS matrix, and to define the shuffling/mapping of the tweak scheduling algorithm and the round constants.<sup>4</sup> Next, we first provide high-level security arguments that justify the

<sup>3</sup> The branch number  $\mathcal{B}$  of a matrix over  $\mathbb{F}_p^t$  is defined as  $\mathcal{B}(M) = \min_{x \in \mathbb{F}_p^t \setminus \{0\}} \{\text{hw}(x) + \text{hw}(M(x))\}$ , where  $\text{hw}(\cdot)$  is denoted as the bundle weight in wide trail terminology. A matrix  $M \in \mathbb{F}_p^{t \times t}$  is an MDS matrix if and only if  $\mathcal{B}(M) = t + 1$ .

<sup>4</sup> Variants where the  $\mathbf{F}$  function uses nearly MDS matrices could be considered.

design choices of FPM ciphers in Section 3. We then propose a first hardware-oriented instance in Section 4 for which we analyze the mathematical security in Section 5 and the implementation efficiency & security in Sections 6 and 7.

### 3 High-level Rationale and Security Arguments

We now provide a high-level rationale and security arguments for  $\text{FPM}_\tau$  TBCs.

#### 3.1 TWEAKEY Framework and LED-like Design

$\text{FPM}_\tau$  ciphers follow the TWEAKEY framework proposed by Jean et al. [78] at Asiacrypt'14. In contrast to the majority of the TBCs following this framework (including SKINNY), we add the tweak only every  $N_\tau > 1$  rounds, where  $N_\tau$  is strictly bigger than 1. This approach is not new in the literature, as it has been already exploited in the block cipher LED [73]. Its main advantage is to allow a very simple security analysis concerning related-tweak attacks.

More precisely, since the tweaks are public, the attacker can always control them. Similar to a related-key attack [18], in a related-tweak attack the attacker encrypts (resp., decrypts) the same or different plaintext(s) (resp., ciphertexts) under several related tweaks. (Anticipating the detailed analysis of Section 5, we emphasize that related-tweak attacks are usually based on statistical properties and not on algebraic ones.) A possible way to avoid such attacks is to treat the tweaks exactly as the plaintexts. That is, not to make any distinction between plaintexts and tweaks. This is what is done in a sponge/duplex construction [14,15], but it requires a larger state in order to arrange the inner part, which is not suitable in our case. Another approach to prevent related-tweak attacks is the one proposed in [73] to prevent related-key attacks. That is, adding the tweak every  $N_\tau > 1$  rounds. The argument for  $\tau = 1$  is relatively simple:

- A statistical attack as the differential one [22,23] exploits the probability distribution of a non-zero input difference leading to an output difference after a given number of rounds. The security is achieved if the probability of any differential characteristic is much smaller than the security level;
- Given  $T \in \mathbb{F}_p^n$ , assume for simplicity that all the  $T_i$ 's  $\in \mathbb{F}_p^n$  are equal to  $T$ ;
- If a difference is inserted in the tweak, then every sub-tweak  $T_i$  will be active;
- Hence, it is impossible to force two consecutive steps  $S$  to be non-active (i.e., with zero input and zero output differences). That is, for every two consecutive steps  $S$  of  $N_\tau$ -rounds, at least one of them must be active.

Indeed, let's assume that the output difference of the  $i$ -th step  $S$  coincide with the difference in  $T_i$ . In this case, the next  $i + 1$ -th step  $S$  is not active, since its input difference is equal to zero. But the next tweak  $T_{i+1}$  will introduce again the difference, making the next  $i + 2$ -th step  $S$  active. Using the number of active steps  $N_s$  (each one composed of  $N_\tau$  rounds), it is therefore possible to provide simple security arguments for preventing differential and other statistical attacks, which reduce to the security of the public permutation  $S$  (which is independent



of the tweaks and the master key). We refer to Appendix B for an initial analysis (based on published results) regarding the selection of the number of steps  $N_s$  independently of their internal structure.

The previous argument can be generalized for a non-trivial tweak scheduling  $T : \mathbb{F}_p^{\tau \cdot n} \equiv (\mathbb{F}_p^n)^\tau \rightarrow (\mathbb{F}_p^n)^*$ , for example if the following properties are satisfied: 1)  $T$  is bijective, and 2)  $T_{j,\cdot} \in \mathbb{F}_p^n$  is active if and only if  $T^{(j)} \in \mathbb{F}_p^n$  is active. Equivalently, this second condition is satisfied if there exist  $\tau$  invertible maps  $T_0, T_1, \dots, T_{\tau-1}$  over  $\mathbb{F}_p^n$  such that  $T_{j,i} = T_j^{i+1}(T^{(j)})$  for each  $i \geq 0$ , where  $T_j^{i+1} := T_j \circ T_j \circ \dots \circ T_j$  for  $i$  times. (We emphasize that this is not a necessary condition.) In our case, we achieve this property by defining  $T_{j,\cdot}$  via a shuffle of the  $\mathbb{F}_p$ -words of  $T^{(j)}$ . (The mapping of each  $\mathbb{F}_p$  does not affect this property.) A detailed argument will be given for **small-pSquare** with  $\tau = 1, 2$  in Section 5.1.

We leave the question whether adding the tweak every round could lead to improved (but harder to analyze) security as a scope for further research.

### 3.2 Rationale behind the Generalized Type-II Feistel Scheme

The main motivation behind the choice of defining  $FPM_\tau$  ciphers based on a generalized Feistel structure relates to the goal of having TBCs with cheap inverses that are useful in some leakage-resistant modes of operation [9,12]. This result can be achieved via 1) a Feistel or Lai-Massey scheme [84,110,67], 2) an SPN scheme with the “reflection” property like Prince [27,29,17], or 3) an SPN scheme in which every round – without the constant additions – is an involution (that is,  $R = R^{-1}$ ) like Noekon [46], Khazad [107] or Iceberg [107]. Even if all options are valid from a security viewpoint, the first one comes with the least constraints on its internal components, which is desirable in our setting in order to enable these components to be selected primarily for their properties against leakage. After discarding Type-I Feistel schemes that require too many rounds for achieving full diffusion, we opted for Type-II generalized Feistel networks instead of Type-III ones. As witnessed by designs like Hight [75] or Clefia [104], they generally offer a good security vs. efficiency compromise.

### 3.3 Rationale and Construction of the Function F

As mentioned in Section 2.3, the F functions aim to ensure good non-linear diffusion while remaining bijective (in order to simplify the security analysis). For functions  $G_{i,j}$  over  $\mathbb{F}_p$  that are themselves bijective, this could be directly obtained with two SPN rounds. Yet, and as mentioned in the introduction, one natural candidate  $G_{i,j}$  function is the square power map, which leads to efficient masked implementations [33]. As a result, we opted for F functions based on two rounds of a generalized Feistel network.<sup>5</sup> We selected the Type-III version which is more similar to SPNs in terms of their number of non-linear  $G_{i,j}$  functions and replaced the middle shift of the  $\mathbb{F}_p$ -words by an invertible linear layer in order to speed up the non-linear diffusion, an idea that resembles the one in [10].

<sup>5</sup> For instances relying on invertible  $G_{i,j}$  functions, we suggest using two SPN rounds.

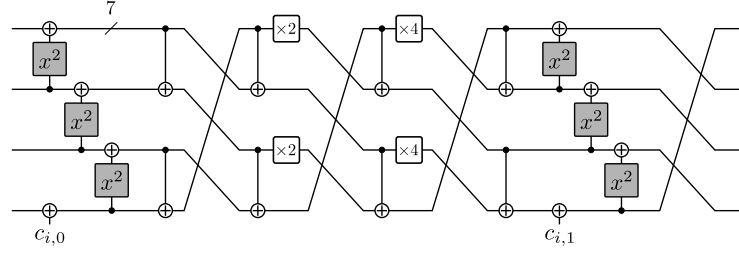


Figure 3: F-function used in small-pSquare.

Regarding the choice of the linear layer, we opted for an MDS matrix which allows to achieve full non-linear diffusion over  $\mathbb{F}_p^c$  in only two rounds. Examples include lightweight candidates [88,82,55] adapted to the prime case (where the multiplication per two can be cheap – see Footnote 2). Such MDS matrices could be replaced by any invertible matrix with a smaller branch number that allows to get full non-linear diffusion in two rounds, as the ones in [87].

Finally, the round constant additions aim to (i) differentiate the rounds (e.g., for preventing slide attacks [24,25]), (ii) break any fixed points, and (iii) break any invariant subspace [85,86,69]. Since  $x \mapsto x^2$  has only two fixed points (namely, 0 and 1) and since  $\mathbb{F}_p$  does not have any non-trivial subspace (as opposed to  $\mathbb{F}_{2^t} \equiv \mathbb{F}_2^t$ ), we believe that one  $\mathbb{F}_p$ -constant addition before each non-linear Type-III generalized Feistel layer is sufficient. As an extra condition when using Mersenne primes, we require that the round constants do not belong to any subspace of  $\mathbb{F}_2^p$  (where  $p = 2^\rho - 1$ ). The choice to generate them via a bit rotation of a fixed mathematical constant like  $\pi$  is for efficient (hardware) implementation purposes. The mathematical constant must be chosen such that all the rotations are in  $\{0, 1, \dots, p-1\}$  where  $p$  is the prime that defines  $\mathbb{F}_p$ .

#### 4 small-pSquare: a Hardware-oriented Instance

In this section, we provide the specifications of a first instance of an  $\text{FPM}_\tau$  cipher. As mentioned in the introduction, its high-level rationale follows two main guidelines. First, we aim to exploit the recently proposed secure squaring gadgets from [33], which were shown to be more efficient than secure multiplications in  $\mathbb{F}_p$ . As a result, we use the square as power map for the  $G_{i,j}$  functions of Section 2.3. Second, we aim to enable efficient hardware implementations. As a result, we use a small Mersenne prime  $p = 2^7 - 1$ . We then propose to use the rounds depicted in the right part of Figure 2, leading to a  $\text{FPM}_\tau(7, 4, 4)$  cipher that provides  $\approx 7 \times 4 \times 4 = 112$  bits of security and we denote as small-pSquare.

We first detail the different components of the function  $F$  (depicted in Figure 3), then finalize the specification of the tweak scheduling algorithm and conclude with the suggested number of rounds per steps and steps.

**Non-Linear Layer.** The non-linear layer of **small-pSquare** is instantiated with the following  $\mathbb{F}_{2^7-1}^4 \rightarrow \mathbb{F}_{2^7-1}^4$  mapping:

$$(x_0, x_1, x_2, x_3) \mapsto (x_0 + x_1^2, x_1 + x_2^2, x_2 + (x_3 + c_{i,j})^2, x_3 + c_{i,j}) \quad ,$$

where  $c_{i,j}$  is a round constant specified thereafter.

**Linear Layer.** The linear layer of **small-pSquare** is instantiated with the invertible matrix  $M \in \mathbb{F}_{2^7-1}^{4 \times 4}$  defined as:

$$M = \begin{bmatrix} 3 & 2 & 1 & 1 \\ 7 & 6 & 5 & 1 \\ 1 & 1 & 3 & 2 \\ 5 & 1 & 7 & 6 \end{bmatrix} .$$

This matrix has been introduced by Duval et al. [55] and is MDS over  $\mathbb{F}_{2^7-1}$ . It can be implemented as a Type-II Feistel-like construction as shown in Figure 3, with only 8 additions and a depth of 4 (which is optimal for 8 additions). We recall that the doubling operation (i.e.,  $x \mapsto 2 \cdot x$ ) modulo a Mersenne prime is just a bit rotation, hence free in hardware and cheap in software.

**Round Constants.** The first 64 bits of the binary sequence of  $\pi$  are (in hexadecimal):  $\pi_{\text{bin64}} = 0\text{x}C90\text{F}DAA22168\text{C}234$ . Let us denote the bit-wise rotation left via  $\ll$ . Then, the left F-function at round  $i$  uses the round constants:

- $c_{i,0} = (\pi_{\text{bin64}} \ll i) \bmod 2^7$ ,
- $c_{i,1} = (\pi_{\text{bin64}} \ll (i + 16)) \bmod 2^7$ ,

while the right F-function at round  $i$  uses the round constants:

- $c_{i,2} = (\pi_{\text{bin64}} \ll (i + 32)) \bmod 2^7$ ,
- $c_{i,3} = (\pi_{\text{bin64}} \ll (i + 48)) \bmod 2^7$ .

As no sequence of 7 consecutive 1s exists in  $\pi_{\text{bin64}}$ , all  $c_{i,0}, c_{i,1}, c_{i,2}, c_{i,3}$ 's  $\in \mathbb{F}_{2^7-1}$ .

**Tweak Scheduling ( $\tau \geq 1$  Only).** Let  $\Pi_{16}$  be the shuffle of the 16  $\mathbb{F}_{2^7-1}$ -words in the tweak schedule sub-tweak word permutation defined as:

$$\Pi_{16}(x_0 \| x_1 \| \dots \| x_{15}) = x_9 \| x_5 \| x_{13} \| x_{15} \| x_{12} \| x_7 \| x_{14} \| x_2 \| x_4 \| x_6 \| x_8 \| x_3 \| x_{10} \| x_1 \| x_{11} \| x_0 .$$

$\Pi_{16}$  has a cycle period of 140 which is the largest we found for 16-element shuffles (and more than sufficient for our envisioned step numbers). On each  $\mathbb{F}_{2^7-1}$ -word, we then apply a bit-shuffle  $\Psi_l$  defined as

$$\forall l \in \{0, 1, \dots, 15\} : \quad \Psi_l(x) = \psi_7(2^l \cdot x \bmod 2^7) ,$$

where the multiplication with  $2^l$  corresponds to a shift of the bits of  $l$  positions (when working over  $\mathbb{F}_2^7$ ), and where  $\psi_7$  is defined as:

$$\psi_7 \left( x = \sum_{i=0}^6 x_i \cdot 2^i \right) = x_0 \cdot 2^5 + x_1 \cdot 2^3 + x_2 \cdot 2^0 + x_3 \cdot 2^4 + x_4 \cdot 2^1 + x_5 \cdot 2^6 + x_6 \cdot 2^2 ,$$

for each  $x \in \mathbb{F}_{2^7-1}$  where  $x_0, x_1, \dots, x_6 \in \{0, 1\}$ . The cycle period of  $\psi_7$  is 12 (i.e., the maximum possible for a permutation over 7 bits). Moreover, the polynomial corresponding to  $\psi_7$  over  $\mathbb{F}_{2^7-1}$  is of degree 125 (i.e., the maximum possible) and contains 46 out of the 127 monomials possible. We refer to Appendix C for details on  $\psi_7$ , where we also prove that the polynomial over  $\mathbb{F}_{2^7-1}$  corresponding to any bit shuffling only contains monomials of odd degree.

**Number of rounds.** For a security level of 112 bits and the aforementioned parameters ( $p = 2^7 - 1; b = 4, c = 4$ ), we use  $N_r = 4$  rounds per step and we use  $N_s = 9$  steps for  $\tau = 0$ ,  $N_s = 16$  steps for  $\tau = 1$  and  $N_s = 21$  steps for  $\tau = 2$ . The security analysis that supports these choices is given in the next section.

## 5 Mathematical Security Analysis of small-pSquare

We now evaluate the security of small-pSquare against standard attack vectors, including classical and truncated differential attacks and algebraic attacks (based on interpolation, linearization, higher-order differentials and Gröbner bases). We describe the attacks having a larger impact on small-pSquare’s number of rounds in the paper. Details of further attacks are presented in Appendix D.

**Overview of the attacks.** As we are going to show, the main attack vector against small-pSquare is differential cryptanalysis [22,23], which we present in detail in Section 5.1 for the case  $\tau = 0$  and the case  $\tau \geq 1$  (for which we consider related-tweak differential attacks). In this last case, we exploit the strategy introduced by the LED designers and recalled in Section 3.1 for guaranteeing security against related tweaks. Truncated [81] and impossible differential [20] cryptanalysis as well as other statistical attacks including linear cryptanalysis [91] and boomerang attacks [113] are detailed in Appendices D.1 and D.2, respectively. Contrary to MPC-/FHE-/ZK-friendly schemes defined over prime fields, and similar to classical/traditional symmetric primitives, algebraic attacks are not the main threat against small-pSquare in our analysis, essentially due to the small size of the prime  $p = 2^7 - 1$  and the high number of variables  $n = 16$ . For this reason, we discuss the degree and density of the polynomial representation of small-pSquare in Section 5.2, limit ourselves to linearization attacks [42] in Section 5.3, while we defer the description of interpolation [77], higher-order differential [83,81] and Gröbner bases based attacks to Appendix D.4.

We mention that in all these cases, we tried to identify concrete strategies on how to speed up the attacks by making use of related tweaks. In particular, we propose concrete ways to use related tweaks for speeding up algebraic attacks which, to the best of our knowledge, has not been thoroughly studied yet in the

open literature.<sup>6</sup> Besides, the non-linear tweak scheduling algorithm of `smallpSquare` is also aimed to frustrate such improved cryptanalysis attempts.

### 5.1 Differential Cryptanalysis

Given pairs of inputs with some fixed input differences, differential cryptanalysis [22,23] considers the probability distribution of the corresponding output differences produced by the cryptographic primitive. Let  $\Delta_I, \Delta_O \in \mathbb{F}_p^n$  be respectively the input and the output differences through a permutation  $P$  over  $\mathbb{F}_p^n$ . The Differential Probability (DP) of having a certain output difference  $\Delta_O$  given a particular input difference  $\Delta_I$  is equal to:

$$\text{Prob}_P(\Delta_I \rightarrow \Delta_O) = \frac{|\{x \in \mathbb{F}_p^n \mid P(x + \Delta_I) - P(x) = \Delta_O\}|}{p^n}.$$

In the case of iterated schemes, a cryptanalyst searches for ordered sequences of differences over any number of rounds that are called differential characteristics/trails. Assuming the independence of the rounds, the DP of a differential trail is the product of the DPs of its one-round differences.

**Differential property of F.** As first step, we compute the maximum differential probability of F. Since  $x \mapsto x^2$  is a quadratic map,  $\text{DP}_{\max}(x \mapsto x^2) = p^{-1} \approx 2^{-7}$ . For our goal, we just need to compute the minimum number of active square maps in F. We can check that it corresponds to 2. Indeed, let  $(x_0, x_1, x_2, x_3) \mapsto (x_0, x_0^2 + x_1, x_1^2 + x_2, x_2^2 + x_3)$  be the Feistel layer, and keep in mind that the branch of the MDS matrix  $M$  is 5. Then:

- If no square map is active in the first Feistel layer of F (hence,  $x_3$  is the only active component), then only one output is active at its output. After the multiplication with the MDS matrix, all inputs of the second Feistel layer are active, which implies the result. A similar result holds if only one square map is active in the first Feistel layer, which corresponds to the case in which only one among  $\{x_0, x_1, x_2\}$  is active. In such a case, two outputs of the first Feistel layer are active, which implies that at least 3 inputs of the second Feistel layer are active and at least 3 square maps are active for each F;
- If two inputs are active, the best scenario for the attacker occurs when the active inputs are either  $\{x_0, x_3\}$  or  $\{x_1, x_3\}$ . In this case, exactly one square map is active in the first Feistel layer (due to the fact that  $x_3$  does not activate any square map), and three outputs of the Feistel layer are active (due to the fact that  $x_0, x_1$  and  $x_3$  are not consecutive). Since the matrix is MDS, then at least two inputs are active for the second Feistel layer, which implies that at least one square map is active in the second Feistel layer. As a result, at least 2 square maps are active for each F;

<sup>6</sup> Binary schemes like AES or SHA-3/Keccak have been shown vulnerable to statistical attacks mainly, while algebraic attacks gain more popularity recently due to the raising of symmetric schemes designed for applications as MPC, FHE, and ZK. Still, symmetric schemes designed for such applications are not tweakable designs.

- If 3 or 4 inputs are active, at least two square maps are active for each  $F$ .

Overall, it directly follows that  $DP_{\max}(x \mapsto F(x)) = p^{-2} \approx 2^{-14}$ .

**Differential property of  $S$ .** As shown in [108,35], at least four consecutive rounds of Type-II generalized Feistel network are necessary to reach full diffusion (i.e.,  $N_r \geq 4$ ). Over 4 consecutive rounds, at least 3 functions  $F$  are active, as shown in Figure 6 in the appendix. As a result, by setting  $N_r = 4$ , it directly follows that  $DP_{\max}(x \mapsto S(x)) \leq DP_{\max}(x \mapsto S(x))^3 \leq p^{-6} \approx 2^{-42}$ .

**Number of steps for security.** Finally, we compute the minimum number of steps  $N_s$  for guaranteeing security. Due to clustering effect (that is, due to the fact that several differential characteristics can be used together for setting up the attack) and due to the possibility to exploit a Meet-in-the-Middle approach for setting up the attack, we claim that the scheme is secure if every differential characteristic has probability smaller than  $2^{-2.5 \cdot \kappa} \approx 2^{-280}$  for an arbitrary factor  $2.5$ ,<sup>7</sup> where  $\kappa = 112 = 7 \cdot 16$  is our target security level. Moreover, we conjecture that the attacker cannot skip more than 2 steps  $S$  by a simple partial key-guessing, since one step  $S$  is sufficient for achieving full diffusion.

*Case:  $\tau = 0$ .* By simple computation, we have  $N_s \geq \lceil 280/42 \rceil + 2 = 7 + 2 = 9$  where 2 steps  $S$  are added for preventing partial key-guessing strategies.

*Case:  $\tau = 1$ .* Following the argument proposed by LED’s designers in [73, Sect. 3] and recalled in Sect. 3.1, the attacker can choose related tweaks such that only one out of two consecutive steps  $S$  is active. As a result, it is sufficient to double the number of steps  $S$  obtained for  $\tau = 0$  to guarantee security. That is,  $N_s \geq 2 \cdot 7 + 2 = 16$ , where we again add 2 steps  $S$  for preventing partial key-guessing.

*Case:  $\tau = 2$ .* In this case, the attacker has more freedom in the choice of the related tweaks. Still, we can adapt the previous security argument as follows. Let us consider separately the next two cases: (i) both  $T^{(0)}$  and  $T^{(1)}$  are active (hence,  $T_{0,i}$  and  $T_{1,i}$  are both active for each  $i \geq 0$  due to the definition of the tweak schedule), and (ii) only one among  $T^{(0)}$  and  $T^{(1)}$  is active (hence, only one among  $T_{0,i}$  and  $T_{1,i}$  is active for each  $i \geq 0$  due to the definition of the tweak schedule). In the first case, the analysis proposed for  $\tau = 1$  applies, which implies that at least one among two consecutive steps  $S$  is active. In the second case, w.l.o.g., we assume that  $T^{(0)}$  is active and  $T^{(1)}$  is inactive. We introduce a “super-step”  $S^2 := S \circ S$  as the application of two consecutive steps  $S$ . By working as before, we can deduce at least one among two consecutive super-steps  $S^2$  is active. Moreover, if a super-step is active, then the two steps  $S$  that compose it are active. Indeed, the fact that  $S^2$  is active implies that  $T_{0,i}$  introduces the difference in the first  $S$ . Its output difference cannot be canceled by  $T_{1,i}$ , which is inactive due to the tweak schedule and due to the assumption. Hence, both steps of  $S^2$  are active. The same result applies if  $T^{(1)}$  is active and  $T^{(0)}$  is inactive.

This reasoning implies that  $N_s \geq 14$  is a necessary condition for security. Yet, we have to keep in mind that the attacker can potentially skip one super-step  $S^2$

<sup>7</sup> We take inspiration on the AES-128, which has  $10 = 2.5 \cdot 4$  rounds, where 4 is the minimum number of rounds for preventing classical differential attacks.

at each side of the cipher by working with input (respectively, output) differences in the plaintexts (resp., ciphertexts) that cancel out with the ones in the tweaks, leading  $S^2$  to be inactive. As a result, we require that  $N_s \geq 2 \cdot 7 + 4 + 2 = 20$ , where we again add 2 steps  $S$  for preventing partial key-guessing.

## 5.2 Degree and Density of the Polynomial Representation

In general, algebraic attacks try to take advantage of the “simple” algebraic description of a scheme for breaking it, where the simplicity can relate (among other properties) to the low degree of the encryption/decryption function, the sparsity of the polynomial representation of such functions, or a particular structure of the algebraic system generated by the cipher. The main ingredient for preventing these attacks is the minimal number of rounds such that the polynomial representations of the cipher have a sufficient degree and too many monomials for the attacks to apply with a complexity lower than  $2^\kappa$ . In this section, we therefore study these two characteristics, pointing out that the encryption function of **small-pSquare** with a fixed key and tweak could be analyzed as a mapping over  $\mathbb{F}_{p^{16}}$  for  $p = 2^7 - 1$ . Nevertheless, since all the operations of  $F$  are at the basis field level (squaring in  $\mathbb{F}_p$ ), the field we consider for the cryptanalyses is  $\mathbb{F}_p$ , and the polynomials built by an adversary belong to  $\mathbb{F}_p[x_0, \dots, x_{15}]/(x_0^p - 1, \dots, x_{15}^p - 1)$ . Note that similar results hold in the context of related tweaks, for which the adversary can consider the same polynomials but with more variables.

**Growth of the degree.** We first focus on the minimal degree that a polynomial in this representation can have, and the number of different monomials that appear in an algebraic system obtainable, after  $r$  rounds. Note that the degree in one variable is at most  $p - 1$ , the total degree is then at most  $16(p - 1)$ , and the total number of monomials is  $p^{16}$ . The degree of  $F$  is  $\deg(F) = 4$ . More precisely, it is 4 in three components and 2 in the last one. The degree of its inverse is  $\deg(F^{-1}) = 8^2 = 2^6$ . Indeed, note that the inverse of the internal function given by  $(y_0, y_1, y_2, y_3) = (x_0 + x_1^2, x_1 + x_2^2, x_2 + x_3^2, x_3)$  is given by  $(x_0, x_1, x_2, x_3) = (y_0 - (y_1 - (y_2 - y_3^2)^2)^2, y_1 - (y_2 - y_3^2)^2, y_2 - y_3^2, y_3)$ .

In both cases ( $F$  and  $F^{-1}$ ), we emphasize that one component of the internal function of  $F$  and  $F^{-1}$  has degree one only. Moreover, in the second case, we emphasize that the degree is different for each output variable, and that only one of them has actually maximum degree 8, and therefore 64 for  $F^{-1}$ . It follows that the degree of a step of  $r$  consecutive rounds  $S$  is  $\deg(S) = \deg(F)^r = 2^{2 \cdot r}$ , where we point out that half of the components have degree 1 at the end of the first round due to the Feistel structure. Accordingly, at round  $r$  two blocks have degree  $\deg(F^{r-1}) = 2^{2 \cdot r - 2}$ . Therefore the minimal degree a polynomial can have after  $r$  rounds is  $2^{2 \cdot r - 3}$  until it reaches the maximum degree. Since the degree of the inverse of a Type-II Feistel scheme is equal to the degree of the Type-II Feistel scheme itself, the same bound applies for  $r$  consecutive steps  $S^{-1}$ .

**Density of the polynomial representation.** While the degree’s growth is an important indicator in order to prevent algebraic attacks, another factor that plays a crucial role is the density of the polynomial representation. Indeed,

various algebraic attacks depend on the number of monomials that appear in the polynomials, which implies that a scheme that admits a sparse polynomial is in general not secure against algebraic attacks even if it is of high degree.

Experimentally, we can verify the number of monomials we obtain in each of the 16 polynomials of a round, but even with simpler versions with a prime smaller than 127 it becomes too complex in practice after a few rounds. For example, even for  $p = 3$ , we observed by practical tests that we already get more than  $2^{16}$  different monomials in some of the polynomials at the end of the third round. Since these experiments are quickly getting impractical, we decided instead to determine the number of rounds for which we expect each polynomial to be dense by considering the following approach. First, we determine  $r_m$  defined as the minimal number of rounds such that at least one complete monomial is present in each one of the 16 polynomials. We denote as complete monomial one monomial  $x^e = \prod_{i=0}^{15} x_i^{e_i}$  such that for each  $i \in [0, 15]$  it holds that  $0 < e_i \leq p-1$  (i.e.,  $x^e$  depends on all the variables). Then, we add the number of rounds such that all possible degrees in one variable can be taken, in other words we add the number of rounds sufficient to wrap over  $p$  (note that the degree in  $x_i$  inside a monomial is always between 0 and  $p-1$  since  $x_i^p = x_i$  over  $\mathbb{F}_p$ ).

We next determine a bound on  $r_m$ . First, due to the Type-II Feistel structure, after 3 rounds not every input has an impact on the 16 outputs, which implies  $r_m > 3$ . Then, we get an upper bound on  $r_m$  based on our experiments (the real value could be smaller, taking the upper bound is conservative). With  $p = 3$  we obtain monomials depending on 10 variables in the polynomials in position 1, 2 and 3 and in positions 9, 10 and 11 by symmetry of the Type-II Feistel structure. These monomials contain all the variables from  $x_0$  to  $x_7$  and  $x_8$  to  $x_{15}$  respectively. Calling X and Y monomials of this shape, we get that at round 5 there are terms of shape X+Y in the polynomials in positions 0, 1, 2, 3, 8, 9, 10 and 11, therefore giving complete monomials after passing through F due to the square operations. Since only half of the input goes through F at each round, one more round is needed to obtain these complete monomials in each position, therefore  $r_m \leq 7$ . When moving to  $p = 2^7 - 1$  we can only observe more monomials (since all the ones with a coefficient multiple of 127 rather than 3 are canceled). Combined with the fact that the degree is at least  $2^{2r-3}$  as shown before, we conclude that 5 extra rounds are sufficient to wrap around  $p$  and reach any degree in one variable. This gives us a bound of 12 rounds (equivalently, three steps S) to expect dense polynomials in the 16 positions.

### 5.3 Linearization Attack

Given a system of polynomial equations, one possible way to solve it is via the linearization technique which works by turning it into a system of linear equations and adding new variables that replace all the monomials in the system of degree larger than 1. The resulting linear system of equations can be solved using linear algebra if there are sufficiently many equations. Consider a system in  $x$  unknowns of degree limited by  $D$ , where the number of monomials  $N(D, x)$  is given by  $N(D, x) = \binom{D+x}{D}$  when  $D < p$ . The attack has a computational cost



of  $\mathcal{O}(N(D, x)^\omega)$  operations (for  $2 < \omega \leq 3$ ), and a memory cost of  $\mathcal{O}(N(D, x)^2)$  to store the linear equations. Depending on parameters' choices, the hybrid approach which combines exhaustive search with this resolution may lead to a reduced cost. Guessing  $l < x$  variables leads to a complexity of:

$$\mathcal{O}(p^l \cdot N(D, x - l)^\omega) .$$

*Case:  $\tau = 0$  (no tweak).* Since the key is composed of 16  $\mathbb{F}_{2^{\tau-1}}$ -words, for any  $l \in [0, 15]$  we computed that  $p^l \cdot N(D, x - l)^\omega > 2^{112}$  occurs already for  $D = 69$  (taking the conservative value of  $\omega = 2$ ). Since the minimal degree follows  $2^{2r-3}$  as shown previously (where  $2^{2r-3} > 2^7 - 1$  for  $r \geq 5$ ), and based on the density analysis just given, we can conclude that 3 steps S (equivalently, 12 rounds) are sufficient to prevent algebraic attacks based on linearization.

*Case:  $\tau \geq 1$  (related tweaks).* The freedom of choosing the tweak(s) can be exploited to cancel some monomials whose coefficients depend on the tweak(s) or part of them. Similarly, the difference of two polynomials under related tweaks can be exploited to cancel monomials whose coefficients are independent of the tweaks. Moreover, the linear combinations of more polynomials under properly chosen related tweaks can be exploited to cancel monomials whose coefficients depend on the tweaks or part of them. In this last case, the attacker has to (i) set up a system of equations in which the linear combinations of the coefficients of some monomials is set to zero, and (ii) solve it (e.g., via linearization or using Gröbner bases) to find the related tweaks that satisfy such conditions.

Obviously, this procedure is not free, since one has to solve equations in the tweak variables that are dense and of high (e.g., maximum) degree. Moreover, the non-linear tweak scheduling must be taken into account as well. Based on the analysis just given (and on the results presented in Appendix D.4 for attacks based on Gröbner bases), it would be infeasible for the attacker to solve a system of equations (in the tweaks instead of the plaintexts) that cover more than 12 rounds (or equivalently 3 steps) of the cipher once the tweak is fully absorbed (where we remind that 12 is the minimum number of rounds for achieving full diffusion in the interpolation polynomial). For this reason, we conjecture that  $12 + 4 \cdot (\tau - 1) = 8 + 4 \cdot \tau$  extra rounds (or  $2 + \tau$ , extra steps, which means 3 or 4 for  $\tau \in \{1, 2\}$ ) are sufficient for preventing related-tweak algebraic attacks. We note that this conjecture does not have to be tight for the security of **small-pSquare** to hold, since we need a larger number of extra steps to prevent related-tweak statistical attacks (respectively, 9 and 12 for  $\tau \in \{1, 2\}$ ).

**Note on Gröbner Bases Attacks.** We recall that Gröbner bases based attacks reduce to linearization attacks when (i) the attacker aims to solve equations linking the plaintexts (and the tweaks) to the ciphertexts only, with the key as only variable, and (ii) the attacker can collect enough data for linearizing the system (i.e., the best scenario for the attacker). Hence, when analyzing the security of our scheme against such attacks in Appendix D.4, we only consider the case in which the system of equations is set up at round level.

## 6 Hardware Performance Evaluation of small-pSquare

In this section we evaluate the hardware cost and performance of the **small-pSquare** instance in comparison to respective implementations of the **SKINNY** lightweight tweakable block cipher [8]. Due to its simple and efficient design, **SKINNY** has gained remarkable popularity in recent years, both in academia and industry, and was selected as part of the ISO/IEC 18033-7:2022 standard for tweakable block ciphers. It has been designed with efficient application of side-channel countermeasures in mind, in particular masking, and is therefore ideally suited for our comparison [8]. Naturally, the general design strategy as well as the individual operations employed by the two ciphers (**small-pSquare** vs. **SKINNY**) are vastly different. At first sight, comparing two primitives with more differences than similarities may appear suboptimal to gain meaningful insights. However, in order to achieve a high level of cost-efficiency, lightweight TBCs necessarily need to be tailored to the amenities of their particular mathematical foundation. Hence, the stark differences between these primitives are a direct manifestation of their specialization to the finite fields they operate in. Only such a comparison can answer the question which mathematical setting (e.g., binary field vs. prime field masking) is preferable for constructing dedicated instances to maximize the efficiency vs. security tradeoff of protected TBC implementations.

Table 1: Cost and performance of round-based unprotected **SKINNY-128** and **small-pSquare** hardware implementations evaluated in TSMC 65 nm technology at typical operating conditions for 100 MHz and 250 MHz clock frequency.

Cipher	Block Size	Key Size	Tweak Size	Freq. [MHz]	Crit. Path [ns]	Area [GE]	Power [mW]	Latency [cyc/enc]
<b>SKINNY</b>	128	128	0	100 250	1.877155	2450.75	0.3915	40/1
			128		1.812617	3396.00	0.5613	48/1
			256		1.905185	4353.00	0.7304	56/1
<b>small-pSquare</b>	112	112	0	100	9.777720	9684.75	1.3547	36/1
			112		9.970046	10798.75	1.5424	64/1
			224		9.937350	11989.50	1.6745	84/1
			0	250	3.945602	12407.75	1.7942	36/1
			112		3.971674	14716.50	2.1160	64/1
			224		3.972123	16034.00	2.2392	84/1

**small-pSquare** has been designed to offer competitive performances to common binary lightweight block ciphers when masking is applied. Nevertheless, we begin by comparing its critical path delay, area, power consumption (at 100 MHz operation) and encryption latency to **SKINNY-128** when both are implemented as unmasked round-based hardware circuits in Table 1. All values are post-synthesis results obtained using Synopsys Design Compiler Version O-2018.06-SP4 as a synthesis tool together with the TSMC 65 nm standard cell library at typical operating conditions for two different clock frequencies, 100 MHz and 250 MHz.

The results show that regardless of the tweak size, unmasked SKINNY-128 is significantly more efficient in terms of critical path delay, area footprint and power consumption when compared to unmasked small-pSquare. The encryption latency, which directly corresponds to the number of rounds, is slightly smaller for small-pSquare without tweak compared to SKINNY-128 without tweak. However, for the tweakable variants it is larger in case of small-pSquare. We conclude that when unprotected, and hence for implementation settings where physical attacks are not a concern, small-pSquare is not fully competitive with binary lightweight ciphers in hardware. Yet, as mentioned before, this was not the primary goal of our design effort. Significantly better efficiency in unprotected hardware would have commanded different design choices that, in part, directly oppose to efficiency in masked representation.

We now focus on the more relevant comparison of secure higher-order masked hardware circuits. We have chosen to compare the small-pSquare version with  $\tau = 1$  with SKINNY-128-256 for 2 up to 4 shares (i.e., first- to third-order secure designs). SKINNY-128-256 is the denotation of the SKINNY variant which receives a 128-bit plaintext, 128-bit key and 128-bit tweak (i.e., a 256-bit tweak) as inputs and computes 48 cipher rounds for one encryption or decryption. We recall that small-pSquare with  $\tau = 1$  receives a 112-bit plaintext, 112-bit key and 112-bit tweak as inputs and computes 64 cipher rounds for one encryption or decryption. To put the difference of round numbers in perspective, remember that small-pSquare is a Type-II generalized Feistel design, i.e., each round updates only half of the state. We will see in the next results that with all other factors being equal, masked small-pSquare implementations generally require fewer clock cycles per encryption (sometimes significantly) than masked SKINNY-128-256 implementations, despite the larger number of rounds of the former design.

We have scanned the literature for publicly available securely masked SKINNY-128-256 implementations, with moderate success. The only higher-order masked hardware implementations of tweakable SKINNY-128 we could find have been published in conjunction with [111,103] as part of a study of the leakage resistance of Romulus and other Authenticated Encryption with Associated Data (AEAD) schemes that made it into the finals of NIST’s Lightweight Crypto Competition. The concrete implementation is hence of the SKINNY-128-384+ variant which is used in Romulus and publicly available on GitHub.<sup>8</sup> Please note that the authors have not verified its security properties experimentally. However, it is based on the trivially composable HPC2 masking scheme [32] which eases the extension of gadget security to full-implementation security. We have modified this implementation slightly to make it compute SKINNY-128-256 instead of SKINNY-128-384+, which commanded small changes to the round numbers and tweak schedule. Since this concrete implementation uses a specific implementation of the SKINNY 8-bit S-box that is tailored towards a certain set of optimization goals, we also wanted to include other, more general, masked SKINNY-128 implementations in our comparison. To this end we have employed the Automated Generation of Masked Hardware (AGEMA) tool published at

<sup>8</sup> [https://github.com/uclcrypto/aead\\_modes\\_levelled\\_hw](https://github.com/uclcrypto/aead_modes_levelled_hw)

Table 2: Cost and performance comparison of masked SKINNY-128-256 and small-pSquare ( $\tau = 1$ ) hardware implementations evaluated in TSMC 65 nm technology at typical operating conditions for 100 MHz and 250 MHz clock.

Cipher	Ref.	Par.	Freq. [MHz]	$d$	Pip.	Crit. Path [ns]	Area [GE]	Power [mW]	Latency [cyc/enc]	Random [bit/cyc]		
SKINNY-128-256		128	100 250	2		1.519177	19026.75	2.8547	432/1	128		
				3		1.763878	38828.75	6.2545	432/1	384		
				4		1.839592	65502.00	8.9225	432/1	768		
		[80]			100 250	2	✓	1.566238	58475.50	13.6144	432/9	128
						3	✓	1.801272	94611.50	21.6698	432/9	384
						4	✓	1.882408	137625.50	30.8983	432/9	768
		32	100 250	2		1.743940	9274.50	1.0755	2160/1	32		
				3		1.903482	15999.00	2.0608	2160/1	96		
				4		1.823993	24442.00	8.2697	2160/1	192		
	[111]	128	100 250	2		3.715469	18035.75	2.5276	288/1	32		
				3		3.232731	28740.75	4.1347	288/1	96		
				4		3.849724	41136.75	5.9918	288/1	192		
small-pSquare		100		2		9.845555	21714.50	2.9370	128/1	84		
				3		9.854049	41982.50	5.6533	128/1	210		
				4		9.852280	62587.75	8.4822	128/1	504		
		112			2	✓	9.852014	30730.25	4.4491	128/2	168	
					3	✓	9.854022	65273.00	9.2764	128/2	420	
					4	✓	9.853921	101168.00	14.3426	128/2	1008	
		250		2		3.857306	29438.50	3.7809	128/1	84		
				3		3.861372	52073.50	6.9574	128/1	210		
				4		3.907730	78441.00	10.5274	128/1	504		
	[this]			250	2	✓	3.852503	40414.75	5.5467	128/2	168	
					3	✓	3.857475	77556.50	11.0357	128/2	420	
					4	✓	3.859051	121589.25	17.4111	128/2	1008	
		100			2		9.847473	15332.25	1.9296	256/1	42	
					3		9.851035	27215.75	3.4077	256/1	105	
					4		9.852068	39237.50	4.9897	256/1	252	
		56			2	✓	9.848985	20735.75	2.8794	256/2	84	
					3	✓	9.941982	39958.75	5.5274	256/2	210	
					4	✓	9.851659	59404.75	8.2398	256/2	504	
	250			2		3.855009	20471.00	2.4330	256/1	42		
				3		3.858206	34485.25	4.2527	256/1	105		
				4		3.859086	48511.25	6.1763	256/1	252		
			250	2	✓	3.858980	26823.25	3.5092	256/2	84		
				3	✓	3.858999	48147.50	6.5390	256/2	210		
				4	✓	3.857775	72245.00	9.9639	256/2	504		

Cipher = Evaluation target, either SKINNY-128-256 or small-pSquare ( $\tau = 1$ ).  
Ref. = Reference, i.e., related publication, AGEMA is cited for automatically generated circuits.  
Par. = Parallelism, i.e., size of the state that is operated on in parallel measured in bits.  
Freq. = Synthesis frequency measured in Megahertz (MHz).  
 $d$  = Number of shares, resulting in security order  $d - 1$ .  
Pip. = Design is pipelined (✓) or not ( ).  
Crit. Path = Critical path of the synthesized circuit measured in nanoseconds (ns).  
Area = Area consumption of the synthesized circuit measured in gate equivalents (GE).  
Power = Power consumption of the synthesized circuit measured in milliwatts (mW).  
Latency = Latency of the synthesized circuit measured in clock cycles per encryption(s).  
Random = Fresh randomness consumption measured in bits per clock cycle.

TCHESS 2022 [80] which is able to turn unprotected hardware implementations of cryptographic primitives automatically into securely masked equivalents. We have utilized the tool to autonomously generate masked implementations of SKINNY-128-256 from the source code for unprotected hardware circuits provided by the SKINNY authors on its website as source material.<sup>9</sup> In particular, we translated both, round-based and 32-bit serialized implementations into their masked equivalents based on the HPC2 masking scheme using the Naive processing method (see [80]), as it led to the most suitable results for a comparison. We further generated both pipelined and non-pipelined masked circuits. Given this collection of securely masked SKINNY-128-256 circuits we are now equipped for an in-depth cost and performance comparison to our prime-field TBC.

Analogously to the selected implementations of SKINNY, we created round-based and half-round-based masked hardware circuits of **small-pSquare**. While these implementations operate on the full state (112 bits) and half the state (56 bits) in parallel, respectively, non-linear operations are only applied to 56 and 28 bits in parallel respectively due to the Feistel structure. Hence, the half-round-based implementations compute only one F-function on a 28-bit input at a time, resulting in a similar serialization level (28 vs. 32) compared to the SKINNY equivalent. The circuits are based on the secure and composable prime-field squaring gadgets introduced in [33]. In fact, we even optimized the 4-share gadget in a way that it only needs a single register stage, using similar optimization strategies as for the 2-share and 3-share case presented by the authors of [33]. The pseudo-code for this optimized 4-share gadget is given in Algorithm 1 of Appendix E. The resulting comparison is presented in Table 2. All results are based on post-synthesis estimations obtained using Synopsys Design Compiler and TSMC 65 nm technology at typical operating conditions for two different frequencies, 100 MHz and 250 MHz. The resulting figures for the SKINNY-128-256 circuits are identical for both frequencies due to the short critical path length. For completeness we also provide figures for the more extreme cases of 500 MHz and 1 GHz operation in Appendix F.<sup>10</sup> Based on this collection of cost and performance results, we conclude that **small-pSquare** is indeed able to compete with SKINNY-128-256 when masked in hardware, especially at lower frequencies. The automatically generated hardware circuits of SKINNY need a rather large amount of cycles per round (regardless of the frequency) and are costly when pipelined. At the target frequencies considered in the table ( $\leq 250$  MHz) SKINNY-128-256 is only consistently cheaper in terms of area when non-pipelined serialized implementations are compared. Yet, this advantage in area footprint comes at a steep price, as the encryption latency is larger by a considerable factor. Overall,

<sup>9</sup> <https://sites.google.com/site/skinnycipher/implementation>

<sup>10</sup> More “extreme”, because cryptographic co-processors manufactured in 65 nm technology are rarely clocked at such high frequencies. This is evident for example in research ASICs manufactured in such technology nodes, as reported in <http://asic.ethz.ch/technologies/65.html>. Furthermore, the vast majority of common criteria certified co-processors protected against side-channel attacks do not exceed 200-300 MHz operation (<https://www.commoncriteriaportal.org/products>).

considering the area/power consumption and the latency together, **small-pSquare** often appears preferable. This changes when very high operating frequencies are needed. Then **SKINNY** becomes preferable, as shown in Tables 5 and 6 of Appendix F. In summary, our results show that **small-pSquare** is indeed capable of providing competitive cost and performance results in the envisioned application settings, and even outperforms its competitor consistently when the frequency is sufficiently low.

*Decryption.* Our comparison focuses on encryption-only circuits. However, adding capability for decryption is trivial for **small-pSquare** due to the Feistel structure. The additional cost for multiplexing between addition and subtraction of **F**-function results for the encryption and decryption process falls in the range of a few percent (depending on masking order and parallelization). Adding decryption capability to the **SKINNY** circuits typically requires twice the area.

*Comparison to AES-prime.* We note that **small-pSquare** is also significantly more efficient in hardware compared to **AES-prime** which has been introduced at Eurocrypt 2023 as the first example of a dedicated cipher for prime-field masking [90]. It shares the same block and key size as **small-pSquare**, but is not tweakable. Compared to **AES-prime** our unmasked **small-pSquare** with  $\tau = 0$  is at least 3 times smaller. More importantly, masked **small-pSquare** with  $\tau = 1$  is on average (over the number of shares) 5 times smaller compared to masked **AES-prime** despite the additional tweak input [90]. This implies that masked **small-pSquare** with  $\tau = 0$  requires a more than 5 times smaller area footprint while also executing in fewer clock cycles under the same frequency, constituting a very notable improvement over the state of the art. In addition, we recall that all variants of **small-pSquare** enable efficient decryption, while **AES-prime** does not.

*Area and power consumption.* It is clear that the comparison of the area and power consumption in Table 2 is affected by the different block, key and tweak sizes of the analyzed primitives. Since all those size parameters are smaller for the chosen prime-field design, this fact may tilt the comparison of the implementation size to **small-pSquare**'s advantage. However, we argue that even if normalizing all area and power figures related to **small-pSquare** artificially by, for example, multiplying them with the corresponding size difference factor, namely  $\frac{128}{112} = \frac{8}{7}$ , our conclusions would not change drastically. In order to avoid any confusion we have *not* applied any artificial normalization of our results. We would also like to mention that for cases where 112 bits of security are insufficient, increasing the security level of **small-pSquare** at low additional cost is possible using the trick employed by the **PRINCE** block cipher with whitening keys [27].

*Latency vs. frequency.* **small-pSquare** naturally allows to trade latency in cycles for frequency in Megahertz and vice versa. The considered masked **SKINNY-128-256** implementations offer less flexibility. They always have a very short critical path but require a larger number of cycles due to the type of masked gadgets that are used. In fact, bit-wise masking, where each binary two-input non-linear

gate (e.g., AND, OR, NAND, NOR) is individually replaced by a masked gadget equivalent, enables high frequency operation but requires many register stages to uphold masking security. This is because any secure masked hardware gadget computing a non-linear operation requires at least one register stage (attempts to improve this are usually based on additional specialized hardware assumptions [100,94]). Introducing a register stage for each atomic bit-level gate entails a high overhead in latency of the implementation, but also in area. While this makes masked SKINNY-128-256 well-suited for high frequency operation, it limits its performance in lower frequency and low-latency applications.

*Mild additional constraints.* We note that `small-pSquare` comes with a few additional constraints due to the fact that it operates in a prime field while data is usually encoded in a binary manner. It is however pretty simple to convert a vector of prime field elements into a sequence of bits, by just viewing it as a representation of an integer in basis  $p$ . For `small-pSquare`, the maximum value is worth  $127^{16} - 1$  which can represent 111-bit values (yielding a one-bit loss in the conversion). Similarly, masking `small-pSquare` requires to generate uniformly random prime numbers. Rejection sampling is a viable method (with probability  $1/127$  to reject a value). Using a PRNG that natively operates in  $\mathbb{F}_p$  is an alternative. Eventually, `small-pSquare` would be best integrated in a leakage-resistant mode of operation, which should not raise specific problems since TBC-based constructions like [11] or [103] are field-agnostic. Overall, none of these minor caveats is expected to bring significant overheads.

## 7 Side-Channel Security Assessment of `small-pSquare`

Finally, we evaluate the security of our masked implementations. In particular, we experimentally assess and compare the side-channel resistance of masked `small-pSquare` ( $\tau = 1$ ) and SKINNY-128-256 implementations by measuring their power consumption on an FPGA device and trying to infer the secret key from their side-channel leakage. We focus on pipelined implementations of `small-pSquare` and SKINNY-128-256 for 2, 3 and 4 shares. The serialized circuits constitute a scenario with lower noise, while the parallel ones help to show the differences at slightly higher noise levels, although their side-channel Signal-to-Noise Ratios (SNRs) are not drastically different. Table 7 of Appendix F additionally contains the SCA evaluation results for the `small-pSquare` versions with extra register stages to enable larger maximum frequencies.

*Setup.* For our experiments we use a SAKURA-G FPGA board which houses two Spartan-6 FPGAs serving as controller and device under test, respectively. All designs are operated at 6 MHz clock frequency (for low noise) and their power consumption is measured using a PicoScope 5244D digital sampling oscilloscope at 250 MS/s sampling rate with 12-bit vertical resolution through a Tektronix CT-1 current probe (bandwidth of up to 1 GHz) placed in the power supply path of the target FPGA. Xilinx ISE Version 14.7 is used to synthesize the circuits, with default parameters except the `-keep_hierarchy` attribute set to `yes`.

Table 3: Comparative side-channel evaluation of pipelined masked SKINNY-128-256 and small-pSquare hardware implementations.

Cipher	Par.	CPR	$d$	mean SNR	median SNR	TVLA det. compl.	SASCA compl.
SKINNY-128-256	128	9	2	0.0023	0.0021	71 000	25 000
			3	0.0015	0.0019	811 000	362 000
			4	0.0013	0.0010	57 000 000	29 832 000
	32	45	2	0.0064	0.0048	52 000	6 000
			3	0.0026	0.0028	680 000	157 000
			4	0.0020	0.0016	48 000 000	17 169 000
small-pSquare	112	2	2	0.0021	0.0019	321 000	213 000
			3	0.0032	0.0013	8 040 000	4 002 000
			4	0.0016	0.0011	> 100 000 000	> 100 000 000
	56	4	2	0.0073	0.0031	238 000	45 000
			3	0.0030	0.0025	7 040 000	1 754 000
			4	0.0018	0.0020	> 100 000 000	> 100 000 000

Cipher = Evaluation target, either SKINNY-128-256 or small-pSquare ( $\tau = 1$ ).  
Par. = Parallelism, i.e., size of the state that is operated on in parallel measured in bits.  
CPR = Cycles per round, i.e., latency of one round function computation measured in cycles.  
 $d$  = Number of shares, resulting in security order  $d - 1$ .  
mean SNR = Mean maximum SNR of all S-box/Squaring input shares in the first round.  
median SNR = Median maximum SNR of all S-box/Squaring input shares in the first round.  
TVLA det. compl. = Minimum number of traces to surpass the TVLA detection threshold.  
SASCA compl. = Minimum number of traces to achieve key rank 1 in a SASCA key recovery.

Table 3 summarizes the evaluation results collected for the 12 different masked implementations,  $6 \times$  SKINNY-128-256 and  $6 \times$  small-pSquare. It is apparent from the mean and median side-channel SNRs computed over all first-round 8-bit S-box (SKINNY-128-256) input shares or 7-bit Squaring (small-pSquare) input shares, that the quality of observations an adversary can make of individual words processed in the circuits is quite similar in both cases (binary-field or prime-field cipher). Thus, the noise levels are not expected to significantly impact the following investigation. We have plotted one set of evaluation results in Figure 4 for the concrete example of serialized pipelined implementations with 3 shares. For all 2-, 3- and 4-share implementations respectively, we have first measured 1 million, 10 million and 100 million traces, in a randomly interleaved sequence of measurements for fixed and for random inputs, according to the Test Vector Leakage Assessment (TVLA) methodology [102]. The resulting non-specific t-test results are illustrated in the third row of Figure 4. The implementations satisfy the expected statistical security order in the experiments, as the smallest moment where leakage is detected is equal to the number of shares. The same holds for all evaluated circuits in Table 3. As a next step we performed exemplary key recovery attacks on the most leaking (highest SNR) 8-bit or 7-bit word respectively of the state. In order to extract the most information from the traces and reduce the effective noise level we have employed a profiled horizontal Soft-Analytical Side-Channel Attack (SASCA) [112]. In a first step all relevant intermediate values are profiled over multiple clock cycles to obtain multivariate templates. Next, a Linear Discriminant Analysis (LDA) is used to perform a linear dimensionality reduction which maximizes class separation on



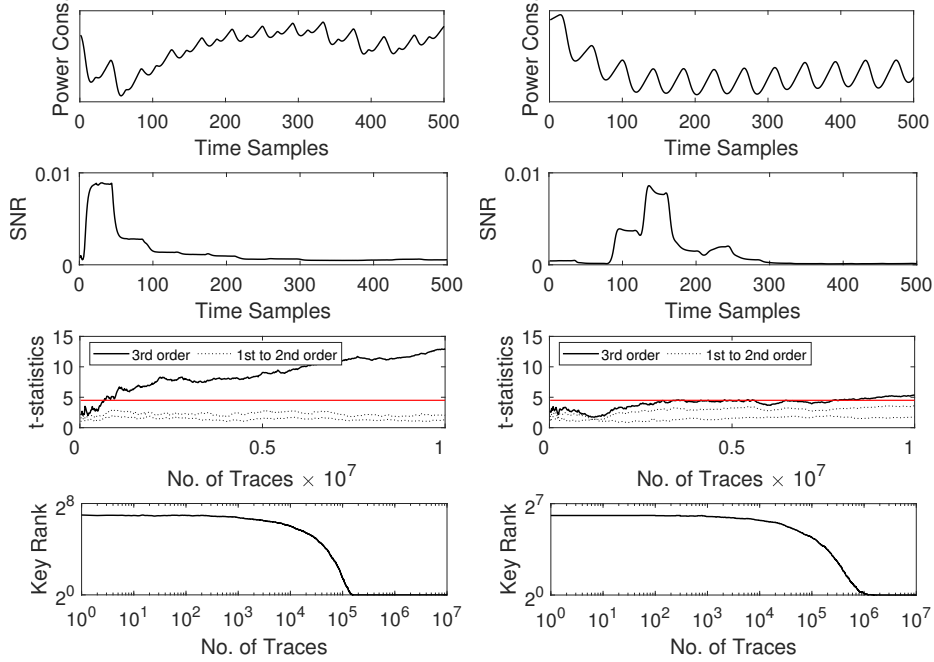


Figure 4: Exemplary SCA results of serialized second-order masked SKINNY-128-256 (left) and small-pSquare (right) hardware implementations. From top to bottom: Sample traces, SNRs (1M traces), Fixed-vs-random t-tests (10M traces), Profiled SASCA (1M profiling, 10M attack traces).

the profiling traces (always 1M) [106]. Finally, on the distinct attack trace set, likelihoods for all intermediate values and corresponding templates are collected separately, before a discrete probability distribution of the secret value is derived using belief propagation inside a SASCA tree graph that contains multiple intermediate computation stages of the masked S-box or squaring. These procedures are readily implemented in the publicly available SCALib library [31]. We then estimate the average rank of the correct key (over 1000 iterations) with the probabilities obtained from all the attack traces. The results of that procedure plotted over the number of attack traces are shown in the bottom row of Figure 4. In both the TVLA and the SASCA results it is apparent that, despite similar SNR values, successful leakage detection and key recovery require consistently significantly more traces (higher data complexity) on the small-pSquare compared to the SKINNY circuits, regardless of the concrete implementation chosen. This advantage of prime-field masking can be attributed to the “algebraic incompatibility” between physical leakage and recombination function to compute the secret from its shares. It can be observed that in case of attacks on 3- and 4-share implementations the advantage of small-pSquare is around or above one order of magnitude (slightly less in case of 2 shares). Furthermore no leakage

detection or sophisticated key recovery attack succeeded on any of the 4-share implementations of `small-pSquare` using 100 million traces. Despite their empirical nature, we believe these results clearly emphasize the interest of efficient TBCs dedicated for prime-field masking based on established design principles (e.g., Feistel structures) while also tailoring the design to specific advantages that a given mathematical structure can lead to (e.g., using squaring as source of non-linearity in prime fields to exploit their efficient masked gadgets).

## 8 Summary and Open Problems

In this paper, we proposed both the FPM family of ciphers that leverages a generalized Feistel structure for prime masking and easy integration in leakage-resistant modes of operation, and the `small-pSquare` instance that is tailored for hardware implementations (due to its small prime) and exploits recent advances for masked squaring gadgets. Combining a hardware performance evaluation with an initial side-channel security assessment allows us to put forward the interest of this approach. `small-pSquare` protected with prime masking shows significantly improved (side-channel) security vs. performance tradeoffs compared to `SKINNY` protected with Boolean masking. Besides their concrete interest, we believe our investigations uncover new design principles for side-channel resistant implementations, leading to new challenges for further research.

Starting from more specific questions, the mathematical and physical security evaluation of `small-pSquare` is, as usual for new ciphers, a natural direction for deeper analyzes. Given the breadth of the FPM family, investigating other instances would be interesting as well. For example, a `mid-pSquare` instance with  $p = 2^{31} - 1$  would be particularly well-suited for software implementations for which masking is known to be difficult to implement due to a lack of noise [7,30]. Such an instance could for example be based on the high-level structure depicted in the left part of Figure 2 combined with the candidate F function given in Figure 5. For modes of operation where having efficient inverses is not critical, it could also be possible to replace the generalized Feistel structure of Section 2.2 by an SPN one. More generally, the use of prime masking raises important theoretical questions regarding security proofs. For example, while the seed results of Dziembowski et al. provide a rationale for prime masking [57], the understanding of this approach is still far from the one of Boolean masking. Typical open problems in this respect are to improve the tightness of the security proofs and to better formalize the intuition of “algebraic incompatibility” that makes prime computations less sensitive to a lack of noise than Boolean masking.

The source code for all our `small-pSquare` implementations is publicly available here: <https://github.com/uclcrypto/small-pSquare>

**Acknowledgments.** Lorenzo Grassi was supported by the German Research Foundation (DFG) within the framework of the Excellence Strategy of the Federal Government and the States – EXC 2092 CaSa – 39078197. Pierrick Méaux

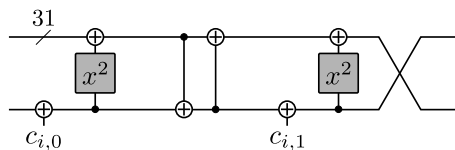


Figure 5: Candidate F-function for a mid-pSquare instance.

was supported by the ERC Advanced Grant 787390. François-Xavier Standaert is a senior research associate of the Belgian Fund for Scientific Research (FNRS-F.R.S.). This work has been funded in parts by the ERC Advanced Grant 101096871. Views and opinions expressed are those of the authors only and do not necessarily reflect those of the European Union or the ERC. Neither the European Union nor the granting authority can be held responsible for them.

## References

1. Martin R. Albrecht, Lorenzo Grassi, Léo Perrin, Sebastian Ramacher, Christian Rechberger, Dragos Rotaru, Arnab Roy, and Markus Schofnegger. Feistel Structures for MPC, and More. In *ESORICS*, volume 11736 of *LNCS*, pages 151–171. Springer, 2019.
2. Martin R. Albrecht, Lorenzo Grassi, Christian Rechberger, Arnab Roy, and Tyge Tiessen. MiMC: Efficient Encryption and Cryptographic Hashing with Minimal Multiplicative Complexity. In *ASIACRYPT*, volume 10031 of *LNCS*, pages 191–219, 2016.
3. Abdelrahman Aly, Tomer Ashur, Eli Ben-Sasson, Siemen Dhooghe, and Alan Szepieniec. Design of Symmetric-Key Primitives for Advanced Cryptographic Protocols. *IACR Trans. Symmetric Cryptol.*, 2020(3):1–45, 2020.
4. Thomas Baignères, Jacques Stern, and Serge Vaudenay. Linear Cryptanalysis of Non Binary Ciphers. In *Selected Areas in Cryptography*, volume 4876 of *LNCS*, pages 184–211. Springer, 2007.
5. Josep Balasch, Sebastian Faust, Benedikt Gierlichs, and Ingrid Verbauwhede. Theory and Practice of a Leakage Resilient Masking Scheme. In *ASIACRYPT*, volume 7658 of *LNCS*, pages 758–775. Springer, 2012.
6. Magali Bardet, Jean-Charles Faugère, Bruno Salvy, and Bo-Yin Yang. Asymptotic behaviour of the degree of regularity of semi-regular polynomial systems. In *Proc. of MEGA*, volume 5, 2005.
7. Alberto Battistello, Jean-Sébastien Coron, Emmanuel Prouff, and Rina Zeitoun. Horizontal Side-Channel Attacks and Countermeasures on the ISW Masking Scheme. In *CHES*, volume 9813 of *LNCS*, pages 23–39. Springer, 2016.
8. Christof Beierle, Jérémy Jean, Stefan Kölbl, Gregor Leander, Amir Moradi, Thomas Peyrin, Yu Sasaki, Pascal Sasdrich, and Siang Meng Sim. The SKINNY Family of Block Ciphers and Its Low-Latency Variant MANTIS. In *CRYPTO*, volume 9815 of *LNCS*, pages 123–153. Springer, 2016.
9. Davide Bellizia, Olivier Bronchain, Gaëtan Cassiers, Vincent Grosso, Chun Guo, Charles Momin, Olivier Pereira, Thomas Peters, and François-Xavier Standaert. Mode-Level vs. Implementation-Level Physical Security in Symmetric Cryptography - A Practical Guide Through the Leakage-Resistance Jungle. In *CRYPTO*, volume 12170 of *LNCS*, pages 369–400. Springer, 2020.

10. Thierry P. Berger, Marine Minier, and Gaël Thomas. Extended Generalized Feistel Networks Using Matrix Representation. In *Selected Areas in Cryptography*, volume 8282 of *LNCS*, pages 289–305. Springer, 2013.
11. Francesco Berti, Chun Guo, Olivier Pereira, Thomas Peters, and François-Xavier Standaert. Tedt, a leakage-resist AEAD mode for high physical security applications. *IACR Trans. Cryptogr. Hardw. Embed. Syst.*, 2020(1):256–320, 2020.
12. Francesco Berti, Chun Guo, Thomas Peters, and François-Xavier Standaert. Efficient Leakage-Resilient MACs Without Idealized Assumptions. In *ASIACRYPT*, volume 13091 of *LNCS*, pages 95–123. Springer, 2021.
13. Francesco Berti, Olivier Pereira, Thomas Peters, and François-Xavier Standaert. On Leakage-Resilient Authenticated Encryption with Decryption Leakages. *IACR Trans. Symmetric Cryptol.*, 2017(3):271–293, 2017.
14. Guido Bertoni, Joan Daemen, Michaël Peeters, and Gilles Van Assche. On the Indifferentiability of the Sponge Construction. In *EUROCRYPT*, volume 4965 of *LNCS*, pages 181–197. Springer, 2008.
15. Guido Bertoni, Joan Daemen, Michaël Peeters, and Gilles Van Assche. Duplexing the Sponge: Single-Pass Authenticated Encryption and Other Applications. In *Selected Areas in Cryptography*, volume 7118 of *LNCS*, pages 320–337. Springer, 2011.
16. Tim Beyne, Anne Canteaut, Itai Dinur, Maria Eichlseder, Gregor Leander, Gaëtan Leurent, María Naya-Plasencia, Léo Perrin, Yu Sasaki, Yosuke Todo, and Friedrich Wiemer. Out of Oddity - New Cryptanalytic Techniques Against Symmetric Primitives Optimized for Integrity Proof Systems. In *CRYPTO*, volume 12172 of *LNCS*, pages 299–328. Springer, 2020.
17. Tim Beyne and Yu Long Chen. Provably Secure Reflection Ciphers. In *CRYPTO*, volume 13510 of *LNCS*, pages 234–263. Springer, 2022.
18. Eli Biham. New Types of Cryptanalytic Attacks Using Related Keys. *J. Cryptol.*, 7(4):229–246, 1994.
19. Eli Biham. A Fast New DES Implementation in Software. In *FSE*, volume 1267 of *LNCS*, pages 260–272. Springer, 1997.
20. Eli Biham, Alex Biryukov, and Adi Shamir. Cryptanalysis of Skipjack Reduced to 31 Rounds Using Impossible Differentials. In *EUROCRYPT*, volume 1592 of *LNCS*, pages 12–23. Springer, 1999.
21. Eli Biham, Orr Dunkelman, and Nathan Keller. The Rectangle Attack - Rectangling the Serpent. In *EUROCRYPT*, volume 2045 of *LNCS*, pages 340–357. Springer, 2001.
22. Eli Biham and Adi Shamir. Differential Cryptanalysis of DES-like Cryptosystems. *J. Cryptol.*, 4(1):3–72, 1991.
23. Eli Biham and Adi Shamir. *Differential Cryptanalysis of the Data Encryption Standard*. Springer, 1993.
24. Alex Biryukov and David A. Wagner. Slide Attacks. In *FSE*, volume 1636 of *LNCS*, pages 245–259. Springer, 1999.
25. Alex Biryukov and David A. Wagner. Advanced Slide Attacks. In *EUROCRYPT*, volume 1807 of *LNCS*, pages 589–606. Springer, 2000.
26. Andrey Bogdanov, Lars R. Knudsen, Gregor Leander, François-Xavier Standaert, John P. Steinberger, and Elmar Tischhauser. Key-Alternating Ciphers in a Provable Setting: Encryption Using a Small Number of Public Permutations. In *EUROCRYPT*, volume 7237 of *LNCS*, pages 45–62. Springer, 2012.
27. Julia Borghoff, Anne Canteaut, Tim Güneysu, Elif Bilge Kavun, Miroslav Knezevic, Lars R. Knudsen, Gregor Leander, Ventzislav Nikov, Christof Paar, Christian

- Rechberger, Peter Rombouts, Søren S. Thomsen, and Tolga Yalçın. PRINCE - A Low-Latency Block Cipher for Pervasive Computing Applications. In *ASIACRYPT*, volume 7658 of *LNCS*, pages 208–225. Springer, 2012.
28. Christina Boura, María Naya-Plasencia, and Valentin Suder. Scrutinizing and Improving Impossible Differential Attacks: Applications to CLEFIA, Camellia, LBlock and Simon. In *ASIACRYPT*, volume 8873 of *LNCS*, pages 179–199. Springer, 2014.
  29. Dusan Bozilov, Maria Eichlseder, Miroslav Knezevic, Baptiste Lambin, Gregor Leander, Thorben Moos, Ventzislav Nikov, Shahram Rasoolzadeh, Yosuke Todo, and Friedrich Wiemer. PRINCEv2 - More Security for (Almost) No Overhead. In *Selected Areas in Cryptography*, volume 12804 of *LNCS*, pages 483–511. Springer, 2020.
  30. Olivier Bronchain and François-Xavier Standaert. Breaking Masked Implementations with Many Shares on 32-bit Software Platforms or When the Security Order Does Not Matter. *IACR Trans. Cryptogr. Hardw. Embed. Syst.*, 2021(3):202–234, 2021.
  31. Gaëtan Cassiers and Olivier Bronchain. Scalib: A side-channel analysis library. *J. Open Source Softw.*, 8(86):5196, 2023.
  32. Gaëtan Cassiers, Benjamin Grégoire, Itamar Levi, and François-Xavier Standaert. Hardware Private Circuits: From Trivial Composition to Full Verification. *IEEE Trans. Computers*, 70(10):1677–1690, 2021.
  33. Gaëtan Cassiers, Loïc Masure, Charles Momin, Thorben Moos, and François-Xavier Standaert. Prime-Field Masking in Hardware and its Soundness against Low-Noise SCA Attacks. *IACR Trans. Cryptogr. Hardw. Embed. Syst.*, 2023(2):482–518, 2023.
  34. Gaëtan Cassiers and François-Xavier Standaert. Trivially and efficiently composing masked gadgets with probe isolating non-interference. *IEEE Trans. Inf. Forensics Secur.*, 15:2542–2555, 2020.
  35. Victor Cauchois, Clément Gomez, and Gaël Thomas. General Diffusion Analysis: How to Find Optimal Permutations for Generalized Type-II Feistel Schemes. *IACR Trans. Symmetric Cryptol.*, 2019(1):264–301, 2019.
  36. Suresh Chari, Charanjit S. Jutla, Josyula R. Rao, and Pankaj Rohatgi. Towards Sound Approaches to Counteract Power-Analysis Attacks. In *CRYPTO*, volume 1666 of *LNCS*, pages 398–412. Springer, 1999.
  37. Shan Chen and John P. Steinberger. Tight Security Bounds for Key-Alternating Ciphers. In *EUROCRYPT*, volume 8441 of *LNCS*, pages 327–350. Springer, 2014.
  38. Jihoon Cho, Jincheol Ha, Seongkwang Kim, ByeongHak Lee, Joohee Lee, Jooyoung Lee, Dukjae Moon, and Hyojin Yoon. Transciphering Framework for Approximate Homomorphic Encryption. In *ASIACRYPT*, volume 13092 of *LNCS*, pages 640–669. Springer, 2021.
  39. Benoit Cogliati, Rodolphe Lampe, and Yannick Seurin. Tweaking Even-Mansour Ciphers. In *CRYPTO*, volume 9215 of *LNCS*, pages 189–208. Springer, 2015.
  40. Benoit Cogliati and Yannick Seurin. Beyond-Birthday-Bound Security for Tweakable Even-Mansour Ciphers with Linear Tweak and Key Mixing. In *ASIACRYPT*, volume 9453 of *LNCS*, pages 134–158. Springer, 2015.
  41. Benoit Cogliati and Yannick Seurin. On the Provable Security of the Iterated Even-Mansour Cipher Against Related-Key and Chosen-Key Attacks. In *EUROCRYPT*, volume 9056 of *LNCS*, pages 584–613. Springer, 2015.
  42. Nicolas T. Courtois, Alexander Klimov, Jacques Patarin, and Adi Shamir. Efficient Algorithms for Solving Overdefined Systems of Multivariate Polynomial

- Equations. In *EUROCRYPT*, volume 1807 of *LNCS*, pages 392–407. Springer, 2000.
43. David Cox, John Little, and Donal O’Shea. *Ideals, varieties, and algorithms: an introduction to computational algebraic geometry and commutative algebra*. Springer Science & Business Media, 2013.
  44. Joan Daemen. Limitations of the Even-Mansour Construction. In *ASIACRYPT*, volume 739 of *LNCS*, pages 495–498. Springer, 1991.
  45. Joan Daemen, Lars R. Knudsen, and Vincent Rijmen. The Block Cipher Square. In *FSE*, volume 1267 of *LNCS*, pages 149–165. Springer, 1997.
  46. Joan Daemen, Michaël Peeters, Gilles Van Assche, and Vincent Rijmen. Nessie Proposal: NOEKEON. First Open NESSIE Workshop, 2000.
  47. Joan Daemen and Vincent Rijmen. The Wide Trail Design Strategy. In *Cryptography and Coding, 8th IMA International Conference 2001*, volume 2260 of *LNCS*, pages 222–238. Springer, 2001.
  48. Joan Daemen and Vincent Rijmen. Security of a Wide Trail Design. In *INDOCRYPT*, volume 2551 of *LNCS*, pages 1–11. Springer, 2002.
  49. Itai Dinur, Orr Dunkelman, Nathan Keller, and Adi Shamir. Key Recovery Attacks on Iterated Even-Mansour Encryption Schemes. *J. Cryptol.*, 29(4):697–728, 2016.
  50. Christoph Dobraunig, Maria Eichlseder, Florian Mendel, and Martin Schl affer. Ascon v1.2: Lightweight Authenticated Encryption and Hashing. *J. Cryptol.*, 34(3):33, 2021.
  51. Christoph Dobraunig, Lorenzo Grassi, Anna Guinet, and Dani el Kuijsters. Ciminion: Symmetric Encryption Based on Toffoli-Gates over Large Finite Fields. In *EUROCRYPT*, volume 12697 of *LNCS*, pages 3–34. Springer, 2021.
  52. Alexandre Duc, Stefan Dziembowski, and Sebastian Faust. Unifying Leakage Models: From Probing Attacks to Noisy Leakage. In *EUROCRYPT*, volume 8441 of *LNCS*, pages 423–440. Springer, 2014.
  53. Alexandre Duc, Sebastian Faust, and Fran ois-Xavier Standaert. Making Masking Security Proofs Concrete - Or How to Evaluate the Security of Any Leaking Device. In *EUROCRYPT*, volume 9056 of *LNCS*, pages 401–429. Springer, 2015.
  54. Orr Dunkelman, Nathan Keller, and Adi Shamir. Minimalism in Cryptography: The Even-Mansour Scheme Revisited. In *EUROCRYPT*, volume 7237 of *LNCS*, pages 336–354. Springer, 2012.
  55. S ebastien Duval and Ga etan Leurent. MDS Matrices with Lightweight Circuits. *IACR Trans. Symmetric Cryptol.*, 2018(2):48–78, 2018.
  56. Stefan Dziembowski and Sebastian Faust. Leakage-Resilient Cryptography from the Inner-Product Extractor. In *ASIACRYPT*, volume 7073 of *LNCS*, pages 702–721. Springer, 2011.
  57. Stefan Dziembowski, Sebastian Faust, and Maciej Sk orski. Optimal Amplification of Noisy Leakages. In *TCC (A2)*, volume 9563 of *LNCS*, pages 291–318. Springer, 2016.
  58. Shimon Even and Yishay Mansour. A Construction of a Cipher from a Single Pseudorandom Permutation. *J. Cryptol.*, 10(3):151–162, 1997.
  59. Jean-Charles Faug ere, Patrizia Gianni, Daniel Lazard, and Teo Mora. Efficient Computation of Zero-dimensional Gr obner Bases by Change of Ordering. 16(4):329–344, 1993.
  60. Jean-Charles Faug ere and Chenqi Mou. Sparse FGLM Algorithms. 80(3):538–569, 2017.
  61. Jean-Charles Faug ere. A new efficient algorithm for computing Gr obner bases ( $F_4$ ). *Journal of pure and applied algebra*, 139(1-3):61–88, 1999.

62. Jean-Charles Faugère. A new efficient algorithm for computing Gröbner bases without reduction to zero ( $F_5$ ). In *Proceedings of the 2002 international symposium on Symbolic and algebraic computation*, pages 75–83, 2002.
63. Guillaume Fumaroli, Ange Martinelli, Emmanuel Prouff, and Matthieu Rivain. Affine Masking against Higher-Order Side Channel Analysis. In *Selected Areas in Cryptography*, volume 6544 of *LNCS*, pages 262–280. Springer, 2010.
64. Jovan Dj. Golic and Christophe Tymen. Multiplicative Masking and Power Analysis of AES. In *CHES*, volume 2523 of *LNCS*, pages 198–212. Springer, 2002.
65. Dahmun Goudarzi and Matthieu Rivain. How Fast Can Higher-Order Masking Be in Software? In *EUROCRYPT*, volume 10210 of *LNCS*, pages 567–597, 2017.
66. Lorenzo Grassi. Mixture Differential Cryptanalysis: a New Approach to Distinguishers and Attacks on round-reduced AES. *IACR Trans. Symmetric Cryptol.*, 2018(2):133–160, 2018.
67. Lorenzo Grassi. On Generalizations of the Lai-Massey Scheme. Cryptology ePrint Archive, Paper 2022/1245, 2022. <https://eprint.iacr.org/2022/1245>.
68. Lorenzo Grassi, Reinhard Lüftenegger, Christian Rechberger, Dragos Rotaru, and Markus Schafneggger. On a Generalization of Substitution-Permutation Networks: The HADES Design Strategy. In *EUROCRYPT*, volume 12106 of *LNCS*, pages 674–704. Springer, 2020.
69. Lorenzo Grassi, Christian Rechberger, and Sondre Rønjom. Subspace Trail Cryptanalysis and its Applications to AES. *IACR Trans. Symmetric Cryptol.*, 2016(2):192–225, 2016.
70. Lorenzo Grassi, Christian Rechberger, and Sondre Rønjom. A New Structural-Differential Property of 5-Round AES. In *EUROCRYPT*, volume 10211 of *LNCS*, pages 289–317, 2017.
71. Hannes Groß, Stefan Mangard, and Thomas Korak. An Efficient Side-Channel Protected AES Implementation with Arbitrary Protection Order. In *CT-RSA*, volume 10159 of *LNCS*, pages 95–112. Springer, 2017.
72. Vincent Grosso, Gaëtan Leurent, François-Xavier Standaert, and Kerem Varici. LS-Designs: Bitslice Encryption for Efficient Masked Software Implementations. In *FSE*, volume 8540 of *LNCS*, pages 18–37. Springer, 2014.
73. Jian Guo, Thomas Peyrin, Axel Poschmann, and Matthew J. B. Robshaw. The LED Block Cipher. In *CHES*, volume 6917 of *LNCS*, pages 326–341. Springer, 2011.
74. Viet Tung Hoang and Phillip Rogaway. On Generalized Feistel Networks. In *CRYPTO*, volume 6223 of *LNCS*, pages 613–630. Springer, 2010.
75. Deukjo Hong, Jaechul Sung, Seokhie Hong, Jongin Lim, Sangjin Lee, Bonseok Koo, Changhoon Lee, Donghoon Chang, Jesang Lee, Kitae Jeong, Hyun Kim, Jongsung Kim, and Seongtaek Chee. HIGHT: A New Block Cipher Suitable for Low-Resource Device. In *CHES*, volume 4249 of *LNCS*, pages 46–59. Springer, 2006.
76. Yuval Ishai, Amit Sahai, and David A. Wagner. Private Circuits: Securing Hardware against Probing Attacks. In *CRYPTO*, volume 2729 of *LNCS*, pages 463–481. Springer, 2003.
77. Thomas Jakobsen and Lars R. Knudsen. The Interpolation Attack on Block Ciphers. In *FSE*, volume 1267 of *LNCS*, pages 28–40. Springer, 1997.
78. Jérémy Jean, Ivica Nikolic, and Thomas Peyrin. Tweaks and Keys for Block Ciphers: The TWEAKEY Framework. In *ASIACRYPT*, volume 8874 of *LNCS*, pages 274–288. Springer, 2014.

79. Stéphanie Kerckhof, François Durvaux, Cédric Hocquet, David Bol, and François-Xavier Standaert. Towards Green Cryptography: A Comparison of Lightweight Ciphers from the Energy Viewpoint. In *CHES*, volume 7428 of *LNCS*, pages 390–407. Springer, 2012.
80. David Knichel, Amir Moradi, Nicolai Müller, and Pascal Sasdrich. Automated Generation of Masked Hardware. *IACR Trans. Cryptogr. Hardw. Embed. Syst.*, 2022(1):589–629, 2022.
81. Lars R. Knudsen. Truncated and Higher Order Differentials. In *FSE*, volume 1008 of *LNCS*, pages 196–211. Springer, 1994.
82. Thorsten Kranz, Gregor Leander, Ko Stoffelen, and Friedrich Wiemer. Shorter Linear Straight-Line Programs for MDS Matrices. *IACR Trans. Symmetric Cryptol.*, 2017(4):188–211, 2017.
83. Xuejia Lai. Higher Order Derivatives and Differential Cryptanalysis. In *Communications and Cryptography: Two Sides of One Tapestry*, pages 227–233. Springer US, 1994.
84. Xuejia Lai and James L. Massey. A Proposal for a New Block Encryption Standard. In *EUROCRYPT*, volume 473 of *LNCS*, pages 389–404. Springer, 1990.
85. Gregor Leander, Mohamed Ahmed Abdelraheem, Hoda AlKhzaimi, and Erik Zenner. A Cryptanalysis of PRINTcipher: The Invariant Subspace Attack. In *CRYPTO*, volume 6841 of *LNCS*, pages 206–221. Springer, 2011.
86. Gregor Leander, Brice Minaud, and Sondre Rønjom. A Generic Approach to Invariant Subspace Attacks: Cryptanalysis of Robin, iSCREAM and Zorro. In *EUROCRYPT*, volume 9056 of *LNCS*, pages 254–283. Springer, 2015.
87. Chaoyun Li and Qingju Wang. Design of Lightweight Linear Diffusion Layers from Near-MDS Matrices. *IACR Trans. Symmetric Cryptol.*, 2017(1):129–155, 2017.
88. Meicheng Liu and Siang Meng Sim. Lightweight MDS Generalized Circulant Matrices. In *FSE*, volume 9783 of *LNCS*, pages 101–120. Springer, 2016.
89. Hamid Mala, Mohammad Dakhilalian, and Mohsen Shakiba. Impossible Differential Attacks on 13-Round CLEFIA-128. *J. Comput. Sci. Technol.*, 26(4):744–750, 2011.
90. Loïc Masure, Pierrick Méaux, Thorben Moos, and François-Xavier Standaert. Effective and Efficient Masking with Low Noise Using Small-Mersenne-Prime Ciphers. In *EUROCRYPT*, volume 14007 of *LNCS*, pages 596–627. Springer, 2023.
91. Mitsuru Matsui. Linear Cryptanalysis Method for DES Cipher. In *EUROCRYPT*, volume 765 of *LNCS*, pages 386–397. Springer, 1993.
92. Florian Mendel, Vincent Rijmen, Deniz Toz, and Kerem Varici. Differential Analysis of the LED Block Cipher. In *ASIACRYPT*, volume 7658 of *LNCS*, pages 190–207. Springer, 2012.
93. Thorben Moos, Amir Moradi, and Bastian Richter. Static power side-channel analysis of a threshold implementation prototype chip. In *DATE*, pages 1324–1329. IEEE, 2017.
94. Rishub Nagpal, Barbara Gigerl, Robert Primas, and Stefan Mangard. Riding the Waves Towards Generic Single-Cycle Masking in Hardware. *IACR Trans. Cryptogr. Hardw. Embed. Syst.*, 2022(4):693–717, 2022.
95. Ivica Nikolic, Lei Wang, and Shuang Wu. Cryptanalysis of Round-Reduced LED. In *FSE*, volume 8424 of *LNCS*, pages 112–129. Springer, 2013.
96. Kaisa Nyberg. Generalized Feistel Networks. In *ASIACRYPT*, volume 1163 of *LNCS*, pages 91–104. Springer, 1996.



97. Santos Merino Del Pozo, François-Xavier Standaert, Dina Kamel, and Amir Moradi. Side-channel attacks from static power: when should we care? In *DATE*, pages 145–150. ACM, 2015.
98. Emmanuel Prouff and Matthieu Rivain. Masking against Side-Channel Attacks: A Formal Security Proof. In *EUROCRYPT*, volume 7881 of *LNCS*, pages 142–159. Springer, 2013.
99. Thomas Roche and Emmanuel Prouff. Higher-order glitch free implementation of the AES using Secure Multi-Party Computation protocols - Extended version. *J. Cryptogr. Eng.*, 2(2):111–127, 2012.
100. Pascal Sasdrich, Begül Bilgin, Michael Hutter, and Mark E. Marson. Low-Latency Hardware Masking with Application to AES. *IACR Trans. Cryptogr. Hardw. Embed. Syst.*, 2020(2):300–326, 2020.
101. Werner Schindler, Kerstin Lemke, and Christof Paar. A Stochastic Model for Differential Side Channel Cryptanalysis. In *CHES*, volume 3659 of *LNCS*, pages 30–46. Springer, 2005.
102. Tobias Schneider and Amir Moradi. Leakage Assessment Methodology - A Clear Roadmap for Side-Channel Evaluations. In *CHES*, volume 9293 of *LNCS*, pages 495–513. Springer, 2015.
103. Yaobin Shen, Thomas Peters, François-Xavier Standaert, Gaëtan Cassiers, and Corentin Verhamme. Triplex: an Efficient and One-Pass Leakage-Resistant Mode of Operation. *IACR Trans. Cryptogr. Hardw. Embed. Syst.*, 2022(4):135–162, 2022.
104. Taizo Shirai, Kyoji Shibusaki, Toru Akishita, Shiho Moriai, and Tetsu Iwata. The 128-Bit Blockcipher CLEFIA. In *FSE*, volume 4593 of *LNCS*, pages 181–195. Springer, 2007.
105. François-Xavier Standaert. How (Not) to Use Welch’s T-Test in Side-Channel Security Evaluations. In *CARDIS*, volume 11389 of *LNCS*, pages 65–79. Springer, 2018.
106. François-Xavier Standaert and Cédric Archambeau. Using Subspace-Based Template Attacks to Compare and Combine Power and Electromagnetic Information Leakages. In *CHES*, volume 5154 of *LNCS*, pages 411–425. Springer, 2008.
107. François-Xavier Standaert, Gilles Piret, Gaël Rouvroy, and Jean-Jacques Quisquater. FPGA implementations of the ICEBERG block cipher. *Integr.*, 40(1):20–27, 2007.
108. Tomoyasu Suzaki and Kazuhiko Minematsu. Improving the Generalized Feistel. In *FSE*, volume 6147 of *LNCS*, pages 19–39. Springer, 2010.
109. Yukiyasu Tsunoo, Etsuko Tsujihara, Maki Shigeri, Teruo Saito, Tomoyasu Suzaki, and Hiroyasu Kubo. Impossible Differential Cryptanalysis of CLEFIA. In *FSE*, volume 5086 of *LNCS*, pages 398–411. Springer, 2008.
110. Serge Vaudenay. On the Lai-Massey Scheme. In *ASIACRYPT*, volume 1716 of *LNCS*, pages 8–19. Springer, 1999.
111. Corentin Verhamme, Gaëtan Cassiers, and François-Xavier Standaert. Analyzing the Leakage Resistance of the NIST’s Lightweight Crypto Competition’s Finalists. In *CARDIS*, volume 13820 of *LNCS*, pages 290–308. Springer, 2022.
112. Nicolas Veyrat-Charvillat, Benoît Gérard, and François-Xavier Standaert. Soft Analytical Side-Channel Attacks. In *ASIACRYPT*, volume 8873 of *LNCS*, pages 282–296. Springer, 2014.
113. David A. Wagner. The Boomerang Attack. In *FSE*, volume 1636 of *LNCS*, pages 156–170. Springer, 1999.

- 114. Lei Wang, Jian Guo, Guoyan Zhang, Jingyuan Zhao, and Dawu Gu. How to Build Fully Secure Tweakable Blockciphers from Classical Blockciphers. In *ASIACRYPT*, volume 10031 of *LNCS*, pages 455–483, 2016.
- 115. Weijia Wang, Pierrick Méaux, Gaëtan Cassiers, and François-Xavier Standaert. Efficient and Private Computations with Code-Based Masking. *IACR Trans. Cryptogr. Hardw. Embed. Syst.*, 2020(2):128–171, 2020.
- 116. Yuliang Zheng, Tsutomu Matsumoto, and Hideki Imai. On the Construction of Block Ciphers Provably Secure and Not Relying on Any Unproved Hypotheses. In *Advances in Cryptology - CRYPTO 1989*, volume 435 of *LNCS*, pages 461–480. Springer, 1989.

### A Active F functions

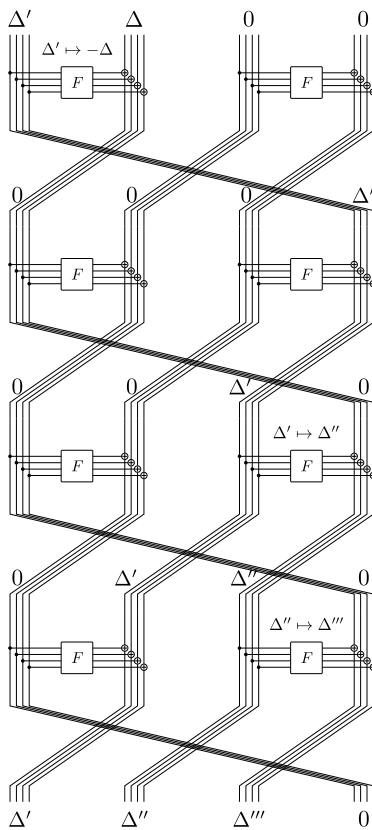


Figure 6: Example of minimum number of active F functions over 4 rounds.

## B High-Level (Provable) Security of FPM TBCs

In this section, we recall a number of results that drive the selection of the number of steps  $N_s$  independent of the internal structure of these steps.

**Case:  $\tau = 0$ .** The cipher  $\text{FPM}_0$  is a typical example of an iterated Even-Mansour (EM) scheme [58]. In their paper, Even and Mansour showed that the security of a 1-round 2-key EM scheme  $\mathbf{E}_{k_0, k_1}(x) := k_1 \oplus \mathbf{P}(x \oplus k_0)$  for a permutation  $\mathbf{P}$  over  $\mathbb{F}_2^n$  is at most of  $n/2$  bits. Since the security provided by a 1-round 2-key EM is much smaller than the  $2^{2n}$  time complexity of exhaustive key search, multiple papers published in the last couple of years have studied the security of iterated EM schemes with more than one round [44,54,26,95,37,49]:

- Bogdanov et al. [26] showed that the  $r$ -round EM scheme with independent keys and permutations and at least  $r \geq 2$  rounds provides security up to approximately  $2^{2n/3}$  queries, but can be broken in  $r \cdot 2^{r \cdot n / (r+1)}$  queries. This bound has been proven to be tight by Chen and Steinberger [37];
- Daemen [44] described a differential chosen-plaintext attack that recovers the key of 1-round EM scheme in approximately  $2^{n/2}$  queries. Later on, Dinur et al. [49] proved that at least 4 rounds are necessary to provide full key-recovery security for an iterated EM scheme with identical sub-keys.

**Case:  $\tau \geq 1$ .** In the case  $\tau \geq 1$ , the attacker can speed up the attacks by exploiting related tweaks. In the TWEAKEY framework in which a tweakkey is used as the key material, several related-tweak attacks can be seen/described as related-key attacks on the EM scheme, since the difference in the sub-key can be simply seen as the difference in the sub-tweak. In [26], Bogdanov et al. remarked that related-key distinguishing attacks against the iterated EM scheme with independent round keys “exist trivially”, and described a related-key key-recovery attack against the two-round EM scheme with identical round keys requiring roughly  $2^{n/2}$  queries (e.g., the 1-round EM scheme satisfies  $\mathbf{E}_{k_0, k_1}(x) = \mathbf{E}_{k_0 \oplus \delta, k_1}(x \oplus \delta)$ , which only holds with negligible probability for an ideal cipher).

In [92], Mendel et al. describe how to extend Daemen’s attack [44] on the EM scheme to a related-key version on iterated EM constructions. For iterated EM with independent sub-keys, they showed that Daemen’s attack can be generalized to yield a related-key attack on  $r$  rounds with complexity of  $\mathcal{O}(r \cdot 2^{n/2})$  (where  $n$  is the sub-key size). More interestingly for our purpose, for iterated EM with identical sub-keys, Mendel et al. showed that Daemen’s attack can be used to break two rounds with complexity of  $\mathcal{O}(2^{n/2})$  in the related-key model.<sup>11</sup> Besides that, they also presented some attacks in the single-key and related-key models, which assume that some of the internal permutations exhibit a high probability differential characteristic (that is, much bigger than  $2^{-n}$ ). In particular, if a

<sup>11</sup> For completeness, we mention a similar related-tweak attack has been presented later on by Cogliati et al. [40] for the case of tweakable EM ciphers with linear tweak schedule.

differential characteristic with probability  $0 < \rho < 1$  exists for (at least) one of the internal permutations, then they show a related-key attack on a 4-round EM scheme instantiated with identical sub-keys with complexity  $\mathcal{O}(2^{n/2} \cdot \rho^{-1/2})$ . The attack is described in Figure 7, where the initial difference  $\Delta_I$  is equal to

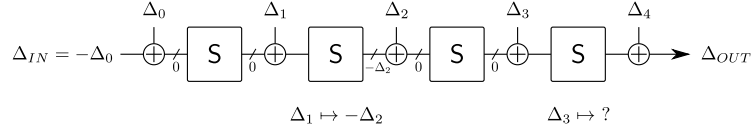


Figure 7: Attack on 4-round EM with related tweaks.

the difference in the first sub-key  $\Delta_0$ , and where the differential trail  $\Delta_1 \rightarrow \Delta_2$  holds with probability  $\rho$  for  $\mathcal{S}$ . It is trivial to note that the previous attack works exactly in the same way in our context in the case  $\tau = 1$ , assuming the difference is not in the key but in the tweak. For the case  $\tau = 2$ , the previous attack can be easily extended to 5 rounds by exploiting the freedom in the second sub-tweak (since it is independent of the first one, the attacker can impose a zero difference in there). Moreover, we point out that the existence of a high probability differential allows the attacker to cover more rounds.

We finally mention that the security of tweakable EM schemes was studied by Cogliati et al. in [41,39], but such results do not apply to our scenario either due to stronger tweak scheduling they considered (based on a hash function) or due to the different size of the key and of tweak with respect to the ones considered in our project.

## C Details about $\Psi_7$

In this part first we show that the polynomial over  $\mathbb{F}_{2^{\rho}-1}$  corresponding to any bit shuffle only contains monomials of odd degree. Then, we give more details on  $\Psi_7$ , the particular bit shuffle we chose and its inverse  $\Psi_7^{-1}$ . Finally we show that  $\Psi_7$  has maximal period.

### C.1 Bit shuffle and odd functions over Mersenne-Prime fields

A bit shuffling is a non-linear operation over  $\mathbb{F}_p$ , where  $p$  is a Mersenne prime. This allows us to set up a non-linear tweak schedule that could help to prevent related-tweak algebraic attacks. From this point of view, we present the following result:

**Proposition 1.** *Let  $p = 2^\rho - 1 \geq 3$  be a prime integer. Let  $\lambda : \mathbb{F}_p \rightarrow \hat{\mathbb{F}}_2^\rho$ , where  $\mathbb{F}_p$  is identified to  $\{0, \dots, p-1\}$  and  $\hat{\mathbb{F}}_2^\rho$  is  $\mathbb{F}_2^\rho$  where  $[0, \dots, 0]$  and  $[1, \dots, 1]$  are identified, be defined as*

$$\lambda \left( x = \sum_{i=0}^{\rho-1} x_i \cdot 2^i \right) = x_0 \| x_1 \| \dots \| x_{\rho-1},$$

where  $x_0, x_1, \dots, x_{\rho-1} \in \{0, 1\}$ . Let  $\Lambda$  be a linear function over  $\mathbb{F}_2^\rho$  such that  $\Lambda([1, 1, \dots, 1]) = [1, 1, \dots, 1]$ . The algebraic polynomial corresponding to  $\mathcal{L}(\cdot) := \lambda^{-1} \circ \Lambda \circ \lambda(\cdot)$  (formally the algebraic normal form of the  $p$ -ary function  $\mathcal{L}$ ), does not contain monomials of even degree (equivalently, it is an odd function, that is,  $\mathcal{L}(x) = -\mathcal{L}(-x)$  for each  $x \in \mathbb{F}_p$ ).

*Proof.* Given  $\lambda(x) = [x_0, x_1, \dots, x_{\rho-1}]$ , for  $x \neq 0$  we have  $\lambda(-x) = \lambda(p - x) = [1 \oplus x_0, 1 \oplus x_1, \dots, 1 \oplus x_{\rho-1}]$ . For  $x = 0$  we have  $\lambda(-x) = \lambda(0) = [0, 0, \dots, 0]$ . It follows that, for  $x \neq 0$

$$\begin{aligned} \mathcal{L}(x) + \mathcal{L}(-x) &= \lambda^{-1} \circ \Lambda \circ \lambda(x) + \lambda^{-1} \circ \Lambda \circ \lambda(-x) \\ &= \lambda^{-1} \circ \Lambda([x_0, x_1, \dots, x_{\rho-1}]) \oplus \lambda^{-1} \circ \Lambda([1 \oplus x_0, 1 \oplus x_1, \dots, 1 \oplus x_{\rho-1}]) \\ &= \lambda^{-1} \circ \Lambda([x_0, x_1, \dots, x_{\rho-1}] \oplus [1 \oplus x_0, 1 \oplus x_1, \dots, 1 \oplus x_{\rho-1}]) \\ &= \lambda^{-1} \circ \Lambda([1, 1, \dots, 1]) = \lambda^{-1}([1, 1, \dots, 1]) = \lambda^{-1}([0, 0, \dots, 0]) = 0. \end{aligned}$$

For  $x = 0$ , since  $\Lambda$  is linear,  $\mathcal{L}(x) + \mathcal{L}(-x) = 2\lambda^{-1} \circ \Lambda \circ \lambda(0) = 2\lambda^{-1} \circ \Lambda([0, \dots, 0]) = 2\lambda^{-1} \circ [0, \dots, 0] = 0$ .

Since  $\mathcal{L}$  is an odd function (that is,  $\mathcal{L}(x) + \mathcal{L}(-x) = 0$  for each  $x \in \mathbb{F}_p$ ),  $\mathcal{L}(x)$  has only monomials with odd degrees as a polynomial over  $\mathbb{F}_p$ , that is,

$$\forall x \in \mathbb{F}_p : \sum_{1 \leq i=2 \cdot i'+1 \leq p-1} \alpha_i \cdot x^i = 0$$

for  $\alpha_i \in \mathbb{F}_p$ . □

Since a bit shuffle is a linear operation, then the polynomial representation of  $\Psi_l$  defined in Section 4 contains only monomials of odd degree.

## C.2 Polynomial Expression of $\Psi_7$ and $\Psi_7^{-1}$

The polynomial corresponding to  $\Psi_7$  over  $\mathbb{F}_{2^7-1}$  is

$$\begin{aligned} \Psi_7(x) &= 6 \cdot x^{125} + 60 \cdot x^{123} + 7 \cdot x^{121} + 42 \cdot x^{117} + 15 \cdot x^{115} + 85 \cdot x^{111} \\ &\quad + 29 \cdot x^{109} + 49 \cdot x^{107} + 71 \cdot x^{103} + 56 \cdot x^{101} + 59 \cdot x^{97} + 62 \cdot x^{95} \\ &\quad + 51 \cdot x^{93} + 12 \cdot x^{89} + 75 \cdot x^{87} + 29 \cdot x^{83} + 120 \cdot x^{81} + 100 \cdot x^{79} \\ &\quad + 37 \cdot x^{75} + 45 \cdot x^{73} + 63 \cdot x^{69} + 61 \cdot x^{67} + 67 \cdot x^{65} + 43 \cdot x^{61} \\ &\quad + 13 \cdot x^{59} + 108 \cdot x^{55} + 106 \cdot x^{53} + 87 \cdot x^{51} + 82 \cdot x^{47} + 8 \cdot x^{45} \\ &\quad + 77 \cdot x^{41} + 95 \cdot x^{39} + 111 \cdot x^{37} + 29 \cdot x^{33} + 85 \cdot x^{31} + 49 \cdot x^{27} \\ &\quad + 28 \cdot x^{25} + 72 \cdot x^{23} + 2 \cdot x^{19} + 51 \cdot x^{17} + 83 \cdot x^{13} + 70 \cdot x^{11} \\ &\quad + 87 \cdot x^9 + 95 \cdot x^5 + 67 \cdot x^3 + 50 \cdot x, \end{aligned}$$

while the polynomial corresponding to  $\Psi_7^{-1}$  over  $\mathbb{F}_{2^7-1}$  is

$$\begin{aligned} \Psi_7^{-1}(x) = & 6 \cdot x^{125} + 86 \cdot x^{123} + 86 \cdot x^{121} + 76 \cdot x^{117} + 40 \cdot x^{115} + 85 \cdot x^{111} \\ & + 122 \cdot x^{109} + 94 \cdot x^{107} + 68 \cdot x^{103} + 107 \cdot x^{101} + 59 \cdot x^{97} + 55 \cdot x^{95} \\ & + 46 \cdot x^{93} + 58 \cdot x^{89} + 73 \cdot x^{87} + 29 \cdot x^{83} + 45 \cdot x^{81} + 13 \cdot x^{79} \\ & + 73 \cdot x^{75} + 120 \cdot x^{73} + 63 \cdot x^{69} + 7 \cdot x^{67} + 43 \cdot x^{65} + 102 \cdot x^{61} \\ & + 77 \cdot x^{59} + 108 \cdot x^{55} + 8 \cdot x^{53} + 71 \cdot x^{51} + 100 \cdot x^{47} + 106 \cdot x^{45} \\ & + 77 \cdot x^{41} + 115 \cdot x^{39} + 3 \cdot x^{37} + 119 \cdot x^{33} + 15 \cdot x^{31} + 49 \cdot x^{27} \\ & + 74 \cdot x^{25} + 50 \cdot x^{23} + 52 \cdot x^{19} + 9 \cdot x^{17} + 83 \cdot x^{13} + 58 \cdot x^{11} \\ & + 71 \cdot x^9 + 57 \cdot x^5 + 94 \cdot x^3 + 100 \cdot x. \end{aligned}$$

For  $\Psi_7$  and  $\Psi_7^{-1}$  (and the other order-12 bit shuffles we tried), we observed that the corresponding polynomials over  $\mathbb{F}_{2^7-1}$  never have degrees even (as proven by Proposition 1), multiple of 7 or congruent to 1 modulo 14 except  $x^1$ . Accordingly, they all have 46 terms.

### C.3 Period of $\Psi_7$

Finally, we prove that  $\Psi_7$  has maximum period, in the sense that there is no bit shuffle that requires a higher number of iterations before returning the original input. For doing this, we point out that the shuffle corresponding to  $\Psi_7$ , that is,

$$(0, 1, 2, 3, 4, 5, 6) \longrightarrow (5, 3, 0, 4, 1, 6, 2),$$

can be divided in two independent cycles, that is,

$$(0, 2, 6, 5) \quad \text{and} \quad (1, 4, 3).$$

Hence, its period is  $\text{lcm}(3, 4) = 12$  (where  $\text{lcm}$  refers to 'least common multiple').

Since we aim to avoid fixed points, we have the following situations:

- two cycles of length 2 and a cycle of length 3, which corresponds to a period of  $\text{lcm}(2, 2, 3) = 6$ ;
- a cycle of length 2 and a cycle of length 5, which corresponds to a period of  $\text{lcm}(2, 5) = 10$ ;
- a cycle of length 3 and a cycle of length 4, which corresponds to a period of  $\text{lcm}(3, 4) = 12$ ;
- a single cycle of period 7.

## D Detailed Security Analysis

### D.1 Truncated and Impossible Differential Cryptanalysis

Truncated differential cryptanalysis [81] generalizes differential cryptanalysis in the sense that truncated differentials are differentials where only a part of the

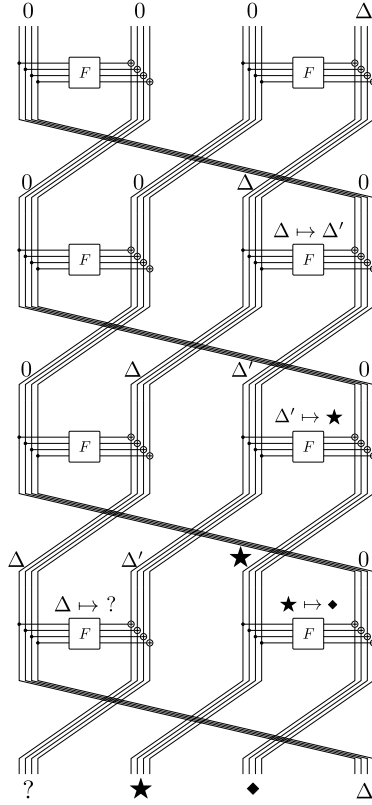


Figure 8: Graphical representation, truncated differential over 4 rounds.

difference can be predicted. That is, the attacker specifies only part of the difference between input texts and lets the remainder take any arbitrary value. Impossible differential attacks [20] exploit output differences which cannot occur in the course of a function (i.e., output differences with probability zero). Impossible differentials are usually set up by concatenating two consecutive truncated differentials that hold with probability 1 and that do not match in the middle.

Let's start by analyzing the single tweak attack scenario. A Type-II Feistel admits the following 4-round truncated differential with probability 1:

$$(0, 0, 0, \Delta) \in (\mathbb{F}_p^4)^4 \mapsto (0, 0, \Delta, 0) \mapsto (0, \Delta, ?, 0) \mapsto (\Delta, ?, ?, 0) \mapsto (?, ?, ?, \Delta) \in (\mathbb{F}_p^4)^4$$

for each  $\Delta \in \mathbb{F}_p^4 \setminus \{0\}$ . Obviously, an analogous truncated differential exists by considering inputs of the form  $(0, \Delta, 0, 0)$ . A graphical representation is provided in Figure 8, where note that  $\star, \blacklozenge \in \mathbb{F}_p^4 \setminus \{0\}$  are non-zero differences since  $F$  is a permutation.

If no shift is applied at the end of  $F$ , it is possible to extend the previous truncated differential to 5 rounds by exploiting the details of  $F$ , as showed in details in Figure 9. We note that the function  $F$  over  $\mathbb{F}_p^4$  admits a truncated

differential with probability 1 of the form

$$(\delta, 0, 0, 0) \in \mathbb{F}_p^4 \mapsto (?, ?, ?, 6 \cdot \delta) \in \mathbb{F}_p^4$$

for each  $\delta \in \mathbb{F}_p \setminus \{0\}$ . However, if no final shift is applied on  $F$ , the truncated differential is of the form

$$(\delta, 0, 0, 0) \in \mathbb{F}_p^4 \mapsto (6 \cdot \delta, ?, ?, ?) \in \mathbb{F}_p^4.$$

In such a case, our design admits a 5-round truncated differential with probability 1 of the form

$$\underbrace{(0, \dots, 0)}_{\in \mathbb{F}_p^{12}}, \delta, 0, 0, 0) \in \mathbb{F}_p^{16} \mapsto (7 \cdot \delta, ?, ?, ?, ?, ?, ?, ?, \delta'_0, \delta'_1, \delta'_2, \delta'_3, ?, ?, ?, ?) \in \mathbb{F}_p^{16}$$

for each  $\delta \in \mathbb{F}_p \setminus \{0\}$ , where  $(\delta'_0, \delta'_1, \delta'_2, \delta'_3) \neq (0, 0, 0, 0)$ . A graphical representation is provided in Figure 9.

By combining two truncated differentials with probability 1, it is possible to set up an impossible differential over 9 rounds of the form

$$(0, 0, 0, \Delta) \xrightarrow[\text{prob. } 1]{\text{RoRoRoR}} (?, \star, \diamond, \Delta) \xrightarrow[\text{prob. } 1]{\text{R}} (?, \diamond, \Delta + \star, ?) \\ \neq (?, ?, \Delta, ?) \xleftarrow[\text{prob. } 1]{\text{R}^{-1} \circ \text{R}^{-1} \circ \text{R}^{-1} \circ \text{R}^{-1}} (0, 0, 0, \Delta),$$

for a certain  $\star \in \mathbb{F}_p^4 \setminus \{0\}$  which is non-zero since  $F$  is a permutation.

Not surprisingly, this is the same impossible truncated differential distinguisher that applies to CLEFIA [104], a Type-2 generalized Feistel over  $\mathbb{F}_{2^{32}}^4$  whose round functions are instantiated with 1-round SPN scheme (that is, one round defined via the concatenation of one S-Box non-linear layer followed by the multiplication with an MDS matrix). Based on this, attacks on 13 rounds CLEFIA have been proposed in the literature [104,109,89,28]. To the best of our knowledge, no other systematic analysis of the impact of (impossible) truncated differential attacks has been performed in the literature. Since 1) we require at least  $N_r \cdot N_s \geq 4 \cdot 9 = 36$  rounds for the security against differential attacks (in the case of a single tweak attack) and since 2) the round function  $F$  of our design (which involves a 2-round Type-III Feistel scheme in which the diffusion is sped up by an MDS matrix multiplication) is not “weaker” than the one of CLEFIA, we conjecture that 36 rounds are sufficient for preventing (impossible) truncated differentials as well.

In a similar fashion, we conjecture that the number of rounds necessary for preventing classical differential attacks in the case  $\tau \in \{1, 2\}$  are sufficient for preventing (impossible) truncated differentials as well.

## D.2 Other Statistical Attacks

We finally claim that the previous number of rounds stated in Section 5.1 provides security against other statistical attacks published in the literature,



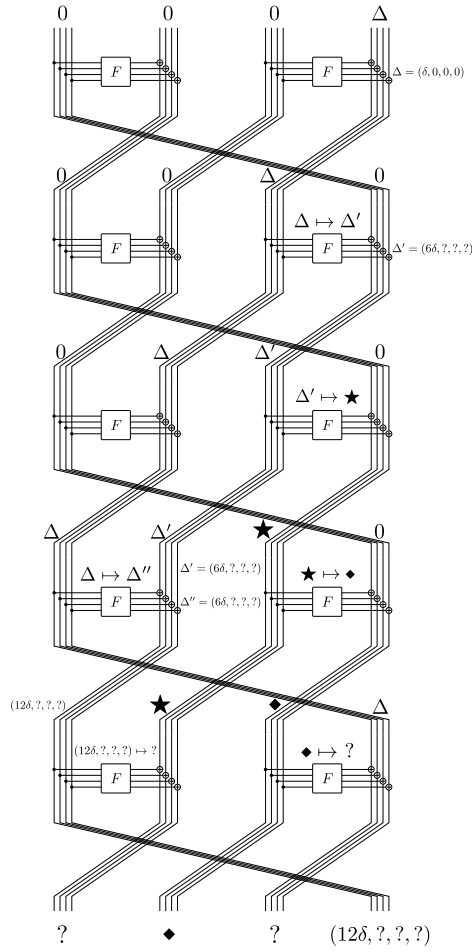


Figure9: Graphical representation, truncated differential over 5 rounds (when no shift is applied).

including (but not limited to) the linearization [91] one and its variants, the boomerang [113] and the rectangle [21] attack, and to structural statistical attacks as the integral [45] one, the multiple-of- $n$  [70] one, and the mixture differential one [66]. We briefly motivate this claim in the following.

In a linear attack, the attacker looks for a linear combination of input, output, and key words that is unbalanced, i.e., biased towards an element of  $\mathbb{F}_p$  with probability higher than  $1/p$  (we refer to [4,51] for more details regarding the linear cryptanalysis over prime fields). In our case, the only non-linear operation is the square map  $x \mapsto x^2$ , which can be approximated by a linear function with probability at most  $2/p$  ( $x^2 = \mu \cdot x$  if and only if  $x \in \{0, \mu\}$ ). Due to this fact and

based on the same analysis proposed for differential attacks proposed before, linear attacks pose no threat against our scheme.

The boomerang attack is a variant of a differential attack which relies on chaining two good differential trails simultaneously. As studied before, any differential characteristic that covers half the number of rounds of our scheme has probability smaller than  $2^{-1.25 \cdot \kappa}$ . It follows that, even if an attacker can find good differentials over a limited number of rounds, it is not possible to set up a boomerang distinguisher/attack on the entire scheme.

Finally, as our scheme works over a prime field, **small-pSquare** could be potentially attacked by all attacks vectors that exploit the strong alignment on symmetric schemes, as the integral and square attacks, or more recently the multiple-of- $n$  differential cryptanalysis and the mixture differential one. However, we claim that such attacks become quickly infeasible, since the nonlinear layer (instantiated via a Feistel scheme) is not aligned and full diffusion is achieved in a single step **S**.

### D.3 Interpolation and Higher Order Differential Attacks

**Interpolation Attack.** In the interpolation attack, the attacker aims to construct the interpolation polynomial that describes the encryption function. With respect to the linearization attack, the variable of such polynomial is the plaintexts (or the ciphertexts) and not the key. Such interpolation polynomial can be exploited to set up attacks, as the forgery attack, a distinguisher one, or a key-recovery attack. E.g., in this last case, the attacker (partially) guesses the final key, sets up the interpolation polynomial on the reduced cipher, and checks it via an extra input/output pair – see [77] for more details. We remark that Meet-in-the-Middle versions of such attack are also possible.

*Case:  $\tau = 0$  (No Tweak).* Since the system of equations over  $\mathbb{F}_p[x_0, \dots, x_{15}]/(x_0^p - 1, \dots, x_{15}^p - 1)$  given by the plaintexts and ciphertexts pairs has the same structure as the one considered previously, we consider again that after 12 rounds (equivalently, 3 steps **S**) we obtain only dense polynomials of maximum degrees. This corresponds to the fact that no adversary can construct the interpolation polynomial with approximately  $2^{112}$  different monomials with a complexity significantly lower than  $2^{112}$ . Since Meet-in-the-Middle versions of such attack are also possible, and since some rounds can be covered by key-guessing (note that 1 step **S** is sufficient for fully absorbing the key), we consider at least  $2 \cdot 12 + 4 = 28$  rounds (or 7 steps **S**) are sufficient for preventing the interpolation attack in the case  $\tau = 0$  (no tweaks).

*Case:  $\tau \geq 1$  (Related Tweaks).* In the case  $\tau \geq 1$  (related tweaks), the attacker can exploit related tweaks to cancel some monomials that appear in the interpolation polynomial. Moreover, the attacker can potentially construct the polynomial whose variables are both the plaintexts and the tweaks. Hence, more data for the attacker means that the attacker can potentially recover a larger number of coefficients of the monomials but at the same time, the number of

monomials grows much faster. Due to the same analysis proposed in Section 5.3, we require at least a number of extra rounds sufficient to get dense polynomials between the addition of two tweaks, that is,  $8 + 4 \cdot \tau$  (that is,  $2 + \tau$  extra steps). Having said that, as for the case of the linearization attack discussed in Section 5.3, related-tweak interpolation attacks do not seem to be as competitive as related-tweak statistical attacks.

**Higher-Order Differential Attack.** The higher-order differential attack has been proposed independently by Lai [83] and by Knudsen [81] for the binary case. Given a function  $F : \mathbb{F}_2^n \rightarrow \mathbb{F}_2$  of degree  $d$ , the attacker exploits the fact that  $\bigoplus_{x \in \mathfrak{V} \oplus \nu} F(x) = 0$  for each  $\nu \in \mathbb{F}_2^n$  and for each subspace  $\mathfrak{V} \subseteq \mathbb{F}_2^n$  of dimension at least equal to  $d + 1$  (that is,  $\dim(\mathfrak{V}) \geq d + 1$ ). For the odd prime case, the result has been recently generalized by Beyne et al. [16] as following. Let  $p \geq 3$  be a prime. Given a function  $F : \mathbb{F}_p^n \rightarrow \mathbb{F}_p$  with degree  $\deg(F) < l \cdot (p - 1)$ , then

$$\sum_{x \in \mathfrak{V} \oplus \nu} F(x) = 0$$

for each  $\nu \in \mathbb{F}_p^n$  and for each subspace  $\mathfrak{V} \subseteq \mathbb{F}_p^n$  of dimension at least  $l$  (remember that  $\mathbb{F}_p$  does not admit any subspace). Therefore an attack with data complexity  $p^l$  can be mounted whenever the degree of  $F$  as a polynomial over  $\mathbb{F}_p$  is strictly less than  $l(p - 1)$ . As usual, such distinguisher can be easily extended into a key-recovery attack, while we are not aware of MitM version of such attack.

*Case:  $\tau = 0$  (No Tweak).* In order to prevent the attack, we ensure that the encryption function has degree at least  $(16 - 1) \cdot (2^7 - 2)$  to ensure a complexity of  $p^{16} \approx 2^\kappa$ . We consider 12 rounds (i.e., 3 steps), to get dense polynomials of maximum degree from the previous analysis. We add 1 extra step due to the possibility for the attacker to cover extra rounds via partial key-guessing.

*Case:  $\tau \geq 1$  (Related Tweaks).* As before, even if the attacker can make use of related tweaks to cancel the monomials of higher degree, the number of rounds necessary for preventing related-tweak statistical attacks are sufficient for preventing related-tweak higher-order differential attacks.

#### D.4 Gröbner Basis Based Attacks

Given a system of multivariate equations, the most efficient methods for solving it over large finite fields involve computing a Gröbner basis associated with the system. We refer to [43] for details on the underlying theory. In the following, we first recall some generic notions about Gröbner basis, and then we estimate the complexity of solving the system of multivariate equations associated to our cipher, first in the case  $\tau = 0$ , and then in the case  $\tau \geq 1$ .

**Theoretical Preliminary.** Given a system of multivariate equations, Gröbner basis algorithms require three steps for solving it:

1. compute the Gröbner basis with respect to *degrevlex* term order with the F4 [61] or F5 [62] algorithm;
2. convert the Gröbner basis into the *lexicographic* term order using the FGLM algorithm [59,60];
3. find the roots of the polynomial system by factoring univariate polynomials and extending the partial solutions.

The complexity depends on several factors, including the number of variables  $n_v$ , the number of equations  $n_e$ , the degree of each equation  $d_0, d_1, \dots, d_{n_e-1} \geq 1$ , and the degree of regularity  $D_{\text{reg}}$ . In order to guarantee the security of our cipher, it is sufficient to show that the cost of (at least) one of the previous steps is higher than  $2^\kappa$  where  $\kappa$  is the security level. In the case  $n_v \leq n_e$ , the complexity of the first step (which is in general the most expensive one) is well estimated by

$$\mathcal{O} \left( \binom{n_v + D_{\text{reg}}}{n_v} \right)^\omega,$$

where  $2 \leq \omega < 3$  is the linear algebra constant, and where the terms hidden by  $\mathcal{O}(\cdot)$  are relatively small (for this reason, in the following analysis, we drop the  $\mathcal{O}(\cdot)$ , and use the expression directly). In general, there does not exist a precise estimation of the degree of regularity for a generic system of equations. However, for the case of a semi-regular system of equations (see e.g. [6] for a formal definition), the degree of regularity is defined as the index of the first non-positive coefficient in the series

$$H(z) = \frac{\prod_{i=0}^{n_e-1} (1 - z^{d_i})}{(1 - z)^{n_v}},$$

where  $d_i$  is the degree of the  $i$ -th equation. If  $n_v = n_e$ , then  $D_{\text{reg}}$  admits a closed formula given by  $D_{\text{reg}} = 1 + \sum_{i=0}^{n_e-1} (d_i - 1)$ .

*Remark 1.* Before going on, we point out that the polynomial systems representing algebraic cryptographic algorithms are often not regular. Since analyzing non-regular systems is very complex in general, a common practice consists in estimating the complexity of the Gröbner basis attack for an equivalent regular system, and to add extra rounds to account for the non-regularity of the system.

### Gröbner Basis Attacks on small-pSquare: Working at Round-Level.

There are many possible ways to represent a cryptographic construction as a system of multivariate polynomials, and this choice impacts the performance of the Gröbner basis algorithm. A first possible way is to set up a system of equations that involves only the known inputs and outputs of the attacked cipher. For small-pSquare, the variables of such system are represented by the secret key words only, and their number is equal to 16. In such a scenario, the attacker

can potentially collect enough polynomials for solving the system of equations by direct linearization, as discussed previously.

Another possible approach consists in working at round level, by introducing new variables and equations for each Feistel layer. While this increases the number of variables, it keeps the degree low. Here, we analyze the security of small-pSquare against this attack, first in the case  $\tau = 0$  (no tweaks), and then in the case  $\tau \geq 1$ .

*Number of Equations and Variables.* The first step for estimating the cost of the Gröbner basis attack consists in setting up the system of equations we aim to solve. Let's start by considering a single input/output. Since the secret key is unknown, it contributes 16 variables. Next, each application of  $F(x_0, x_1, x_2, x_3) = (y_0, y_1, y_2, y_3)$  over  $\mathbb{F}_{2^7-1}^4$  can be described by 6 equations of degree 2 (that is,  $y_0, y_1, y_2$  and the auxiliary variables  $z_1, z_2, z_3$ ) and 1 equation of degree 1 (that is,  $y_3$ ):

$$\begin{aligned} z_1 &= x_0^2 + x_1, & z_2 &= x_1^2 + x_2, & z_3 &= x_2^3 + x_3, \\ y_0 &= (z_3 + z_2 + 2 \cdot z_1 + 3 \cdot x_0)^2 + (z_3 + 5 \cdot z_2 + 6 \cdot z_1 + 7 \cdot x_0), \\ y_1 &= (z_3 + 5 \cdot z_2 + 6 \cdot z_1 + 7 \cdot x_0)^2 + (2 \cdot z_3 + 3 \cdot z_2 + z_1 + x_0), \\ y_2 &= (2 \cdot z_3 + 3 \cdot z_2 + z_1 + x_0)^2 + (6 \cdot z_3 + 7 \cdot z_2 + z_1 + 5 \cdot x_0), \\ y_3 &= z_3 + z_2 + 2 \cdot z_1 + 3 \cdot x_0. \end{aligned}$$

Working over  $r \geq 2$  rounds (remember that each round R is composed of 2 functions F), we have  $12 \cdot r$  equations of degree 2 plus  $2 \cdot r$  equations of degree 1. We can use the intermediate linear equations to eliminate variables, reducing ourselves to  $12 \cdot r$  equations of degree 2 plus 4 final equations of degree 1 (that describe the output of the cipher). The number of variables of this system is  $16 + (12 \cdot r + 4)$ . Since the output of the cipher is assumed to be known, we can use it to eliminate the 16 last variables, reducing ourselves to a system of  $12 \cdot r + 4$  equations in  $12 \cdot r + 4$  variables.

*Over-Determined Case.* In the most general case, one can consider  $m \geq 2$  inputs/outputs. By working as before, one sets up a system of equations composed of  $12 \cdot r \cdot m$  equations of degree 2 and  $4 \cdot m$  equations of degree 1, in  $16 + (12 \cdot r - 12) \cdot m$  variables. Note that the such system is over-determined, since the number of equations  $12 \cdot r \cdot m + 4 \cdot m = 4 \cdot m \cdot (3r + 1)$  is always bigger than the number of variables. However, since the number of variables and equations is much higher than the single input/output case, it is expected that the cost of solving such system is minimized for  $m = 1$ .

*Estimation of the Degree of Regularity.* Working with a single input/output, and assuming the system of equation to be semi-regular, the degree of regularity is given by

$$D_{\text{reg}} = 1 + 12 \cdot r,$$

which is depicted by the green dashed curve in Figure 10. To verify this trend, we have encoded the equations in `sage`, and computed the degree using the `.degree_of_semi_regularity()` method. Our practical tests, depicted by the blue points on Figure 10, suggest however that a good estimation for the degree of regularity is given by  $D_{\text{est}} = 4 \cdot r - 3$ , as given by the light green dotted line. Still, in the following, we will use

$$D_{\text{est}} = 2 \cdot r - 1$$

depicted in Figure 10 by the pink dashed curve, as a more conservative choice.

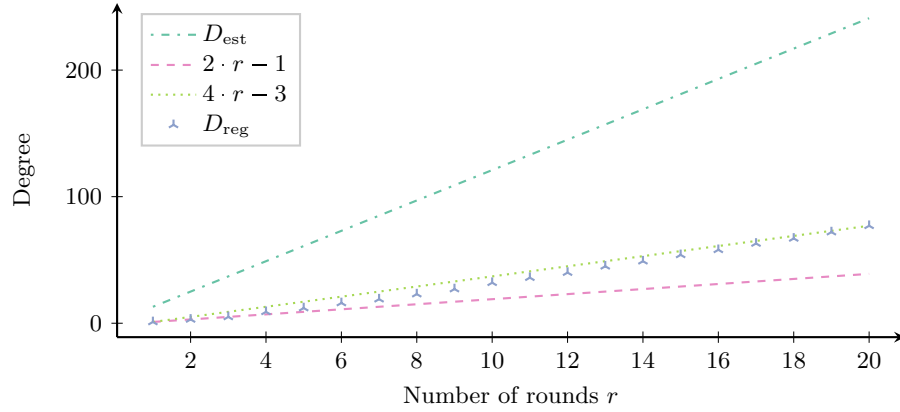


Figure 10: Degree of regularity with respect to the number of rounds: estimations and practical tests.

*Estimation of the Cost of the Gröbner Basis Attack (for  $\tau = 0$ ).* By using  $D_{\text{est}}$ , the cost of the first step of the attack is estimated by

$$\left( \binom{4 + 12 \cdot r + 2 \cdot r - 1}{12 \cdot r + 4} \right)^\omega.$$

Since  $\omega \geq 2$  and since 112 is our security level (in bits), such attack is prevented if

$$\left( \binom{14 \cdot r + 3}{12 \cdot r + 4} \right)^2 \geq 2^{112} \quad \implies \quad r \geq 8,$$

that is, 2 steps S.

In the previous computation, we assumed that the Gröbner basis attack against `small-pSquare` is comparable to that of solving a semi-regular system with  $12r$  quadratic equations + 4 linear equations in  $12r + 4$  variables. However, we note that not all polynomials in our modeling will contain every variable, which adds a certain structure that an attacker might be able to use when reducing

the matrices encountered in F4. We emphasize that we accounted this fact 1) in the conservative choice of using  $\omega = 2$  for the linear algebra constant, 2) in the use of  $D_{\text{est}}$  which is smaller than the results of our practical tests. Finally, the choice  $N_s = 9$  for preventing differential attacks implies a security margin of 7 steps  $S$  (equivalently, 28 rounds) against such attack.

*Case:*  $\tau \geq 1$ . Finally, even if the attack can be potentially sped up by taking into account related tweaks, it seems infeasible that it can be as competitive as other related-tweak attacks discussed before.

## E Single-Cycle 4-Share PINI Squaring Gadget

The masked squaring gadget with 4 shares and a single register stage described by Algorithm 1 is conjectured to be 3-glitch-robust PINI [34].

---

**Algorithm 1** Masked squaring (glitch-robust PINI) with  $d = 4$  shares.

---

**Input:** Sharing  $\mathbf{a}$ .

**Output:** Sharing  $\mathbf{b}$  such that  $b = a^2$ .

---

```

1: for  $i = 0$  to 11 do
2:    $r_i \xleftarrow{\$} \mathbb{F}_p$ 

3:  $\alpha_0 \leftarrow 2\mathbf{a}_1 + r_0$ 
4:  $\alpha_1 \leftarrow 2\mathbf{a}_2 + r_1$ 
5:  $\alpha_2 \leftarrow 2\mathbf{a}_3 + r_2$ 
6:  $\alpha_3 \leftarrow 2\mathbf{a}_0 + r_3$ 
7:  $\alpha_4 \leftarrow 2\mathbf{a}_0 + r_4$ 
8:  $\alpha_5 \leftarrow 2\mathbf{a}_1 + r_5$ 

9:  $\beta_0 \leftarrow \mathbf{a}_0(\mathbf{a}_0 - r_0) + r_6 + r_7$ 
10:  $\beta_1 \leftarrow \mathbf{a}_1(\mathbf{a}_1 - r_1) - r_7 + r_8$ 
11:  $\beta_2 \leftarrow \mathbf{a}_2(\mathbf{a}_2 - r_2) - r_8 + r_9$ 
12:  $\beta_3 \leftarrow \mathbf{a}_3(\mathbf{a}_3 - r_3) - r_9 + r_{10}$ 
13:  $\beta_4 \leftarrow \mathbf{a}_2 r_4 + r_{10} - r_{11}$ 
14:  $\beta_5 \leftarrow \mathbf{a}_3 r_5 + r_{11} + r_6$ 

15:  $\mathbf{b}_0 \leftarrow \text{Reg}(\beta_1) + \mathbf{a}_0 \text{Reg}(\alpha_0)$ 
16:  $\mathbf{b}_1 \leftarrow \text{Reg}(\beta_2) - \text{Reg}(\beta_4) + \mathbf{a}_1 \text{Reg}(\alpha_1)$ 
17:  $\mathbf{b}_2 \leftarrow \text{Reg}(\beta_3) - \text{Reg}(\beta_5) + \mathbf{a}_2(\text{Reg}(\alpha_2) + \text{Reg}(\alpha_4))$ 
18:  $\mathbf{b}_3 \leftarrow \text{Reg}(\beta_0) + \mathbf{a}_3(\text{Reg}(\alpha_3) + \text{Reg}(\alpha_5))$ 

```

---

## F Higher Frequency and Latency Results

Table 4: Cost and performance of round-based unprotected SKINNY-128 and small-pSquare hardware implementations evaluated in TSMC 65 nm technology at typical operating conditions for 500 MHz and 1 GHz clock frequency.

Cipher	Block Size	Key Size	Tweak Size	Freq. [MHz]	Crit. Path [ns]	Area [GE]	Power [mW]	Latency [cyc/enc]
SKINNY	128	128	0	500	1.850039	2450.75	0.3914	40/1
			128		1.812617	3396.00	0.5613	48/1
			256		1.866683	4353.00	0.7306	56/1
			0	1000	0.913763	2835.00	0.4330	40/1
			112		0.957316	3797.75	0.6219	48/1
			224		0.943099	4736.50	0.7765	56/1
small-pSquare	112	112	0	500	1.970174	14382.50	1.8891	72/2
			112		1.965831	16571.25	2.1521	128/2
			224		1.946081	17498.25	2.2782	168/2
			0	1000	0.979052	17217.00	2.4286	144/4
			112		0.977633	19424.25	2.7170	256/4
			224		0.981642	20693.75	2.8573	336/4

Table 5: Cost and performance comparison of masked SKINNY-128-256 and small-pSquare ( $\tau = 1$ ) hardware implementations evaluated in TSMC 65 nm technology at typical operating conditions for 500 MHz clock frequency.

Cipher	Ref.	Par.	$d$	Pip.	Crit. Path [ns]	Area [GE]	Power [mW]	Latency [cyc/enc]	Random [bit/cyc]	
SKINNY-128-256	[80]	128	2		1.519177	19026.75	2.8547	432/1	128	
			3		1.763878	38828.75	6.2545	432/1	384	
			4		1.839592	65502.00	8.9225	432/1	768	
			2	✓	1.566238	58475.50	13.6144	432/9	128	
			3	✓	1.801272	94611.50	21.6698	432/9	384	
			4	✓	1.882408	137625.50	30.8983	432/9	768	
		32	2		1.743940	9274.50	1.0755	2160/1	32	
			3		1.903482	15999.00	2.0608	2160/1	96	
			4		1.823993	24442.00	8.2697	2160/1	192	
			2	✓	1.885406	39016.25	9.1220	2160/9	32	
			3	✓	1.943746	57757.00	13.4186	2160/9	96	
			4	✓	1.909085	78243.00	17.9452	2160/9	192	
	[111]	128	2		1.933508	18035.75	2.5361	288/1	32	
			3		1.944391	28775.50	4.1321	288/1	96	
			4		1.933779	41143.75	5.9978	288/1	192	
			2		1.859616	29862.75	3.5537	320/1	34	
			3		1.955726	52153.25	6.4189	320/1	84	
			4		1.955649	78087.00	9.8462	320/1	202	
small-pSquare	[this]	112	2	✓	1.953954	47786.50	6.7981	320/5	168	
			3	✓	1.906346	87437.50	12.5397	320/5	420	
			4	✓	1.859594	136319.50	19.7666	320/5	1008	
			2		1.955629	21186.50	2.3152	640/1	17	
			3		1.955702	34677.25	3.9515	640/1	42	
			4		1.955738	50638.25	5.9314	640/1	101	
			56	2	✓	1.859584	33663.25	4.6977	640/5	84
				3	✓	1.956702	57478.75	8.3328	640/5	210
				4	✓	1.980931	86320.25	12.1962	640/5	504



Table 6: Cost and performance comparison of masked SKINNY-128-256 and small-pSquare ( $\tau = 1$ ) hardware implementations evaluated in TSMC 65 nm technology at typical operating conditions for a 1 GHz clock frequency.

Cipher	Ref.	Par.	$d$	Pip.	Crit. Path [ns]	Area [GE]	Power [mW]	Latency [cyc/enc]	Random [bit/cyc]	
SKINNY-128-256	[80]	128	2		0.949509	19407.50	2.9036	432/1	128	
			3		0.947323	40094.25	6.4985	432/1	384	
			4		0.954137	67513.25	8.9752	432/1	768	
			2	✓	0.951373	58928.50	13.7255	432/9	128	
			3	✓	0.953803	95915.50	21.9737	432/9	384	
			4	✓	0.950508	139883.75	31.4951	432/9	768	
		32	2		0.955532	9544.50	1.0952	2160/1	32	
			3		0.955728	16525.50	2.1183	2160/1	96	
			4		0.947166	25104.00	8.1450	2160/1	192	
			2	✓	0.950554	39256.75	9.1467	2160/9	32	
			3	✓	0.952657	58274.75	13.5388	2160/9	96	
			4	✓	0.951762	78972.25	18.1421	2160/9	192	
	[111]	128	2		0.953287	19077.50	2.5824	288/1	32	
			3		0.951160	29998.25	4.2289	288/1	96	
			4		0.955633	42781.25	6.1521	288/1	192	
	small-pSquare	[this]	112	2		0.984539	33206.50	4.0781	640/1	17
				3		0.988338	61491.00	7.7516	640/1	42
				4		0.989980	90334.25	11.8584	640/1	101
2				✓	0.974142	61712.75	9.9905	640/10	168	
3				✓	0.930758	114461.25	18.1467	640/10	420	
4				✓	0.982303	158879.25	27.0836	640/10	1008	
56			2		0.988946	24377.25	2.6962	1280/1	9	
			3		0.989175	41025.75	4.7424	1280/1	21	
			4		0.989994	58694.00	7.1102	1280/1	51	
			2	✓	0.930693	46481.75	7.3055	1280/10	84	
			3	✓	0.983510	79853.25	12.3280	1280/10	210	
			4	✓	0.986008	117094.00	18.2342	1280/10	504	

Table 7: Side-channel security evaluation of pipelined masked small-pSquare hardware implementations optimized for higher frequency operation.

Cipher	Par.	CPR	$d$	mean SNR	median SNR	TVLA det. compl.	SASCA compl.
small-pSquare	112	5	2	0.0094	0.0019	417 000	163 000
			3	0.0024	0.0024	9 350 000	6 183 000
			4	0.0020	0.0016	> 100 000 000	> 100 000 000
		10	2	0.0034	0.0021	309 000	188 000
			3	0.0022	0.0018	8 478 000	3 831 000
			4	0.0018	0.0012	> 100 000 000	> 100 000 000
	56	10	2	0.0043	0.0038	229 000	53 000
			3	0.0041	0.0039	7 504 000	1 562 000
			4	0.0036	0.0033	> 100 000 000	> 100 000 000
		20	2	0.0045	0.0052	343 000	42 000
			3	0.0046	0.0036	9 881 000	1 439 000
			4	0.0029	0.0021	> 100 000 000	> 100 000 000